



# Machine Learning Forecast Sensitivity

James D. Doyle<sup>1</sup> and Daniel J. Lloveras<sup>2</sup>

<sup>1</sup>U.S. Naval Research Laboratory, Monterey, CA, <sup>2</sup>SAIC

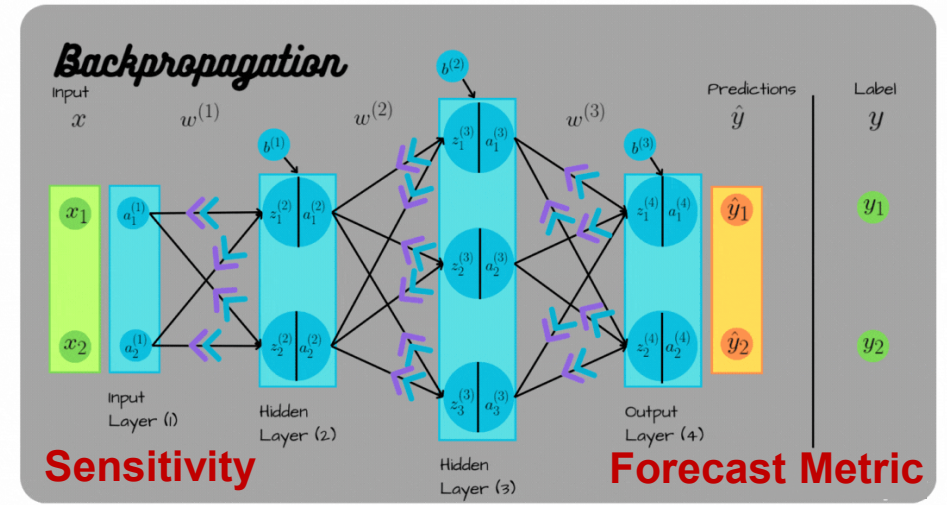
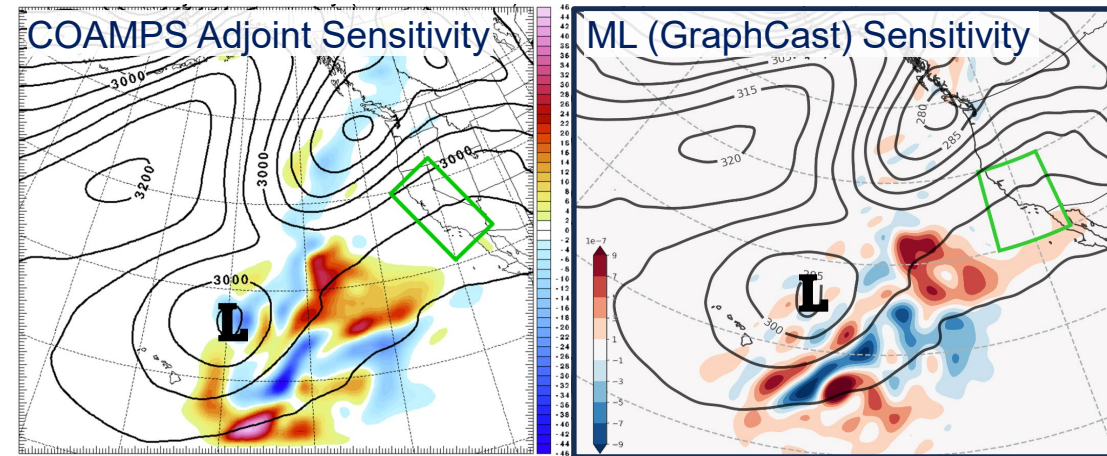
*We acknowledge the support of the NRL Base Program  
Computational support provided by the Navy DoD Supercomputing Resource Center*

*2026 AR Recon Workshop and 2nd Observational Campaigns Workshop for Better Weather Forecasts  
June 29 to July 3, 2026*

*Distribution Statement A. Approved for public release. Distribution is unlimited.*

# Deep Learning Sensitivity Analysis

48-h precipitation sensitivity to the 700-hPa water vapor  
St. Valentine's Day AR and CA Flooding (2019)



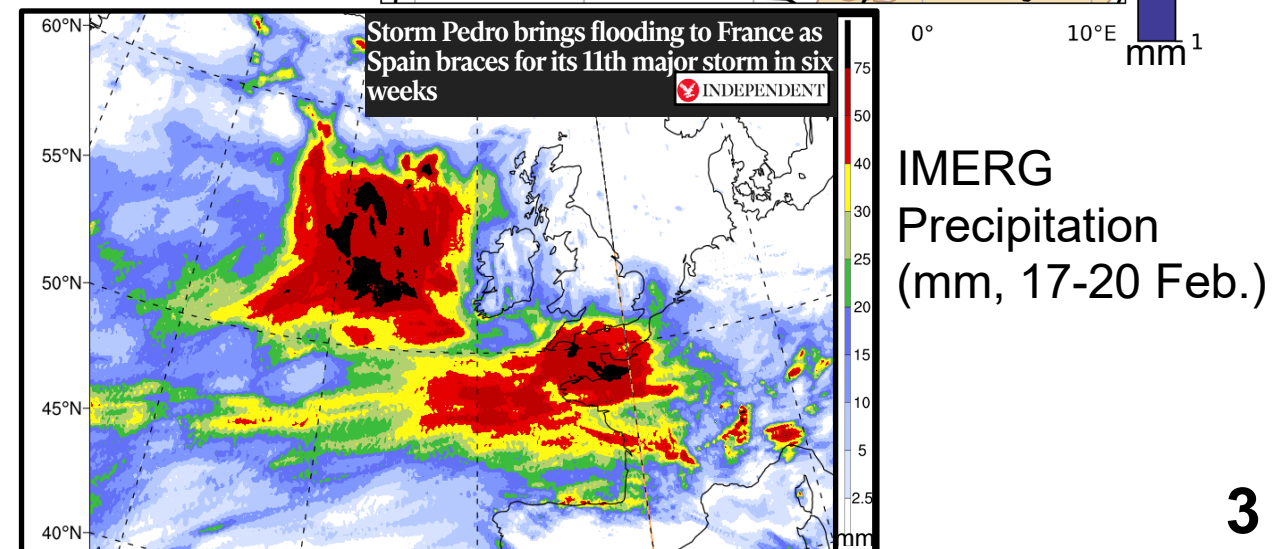
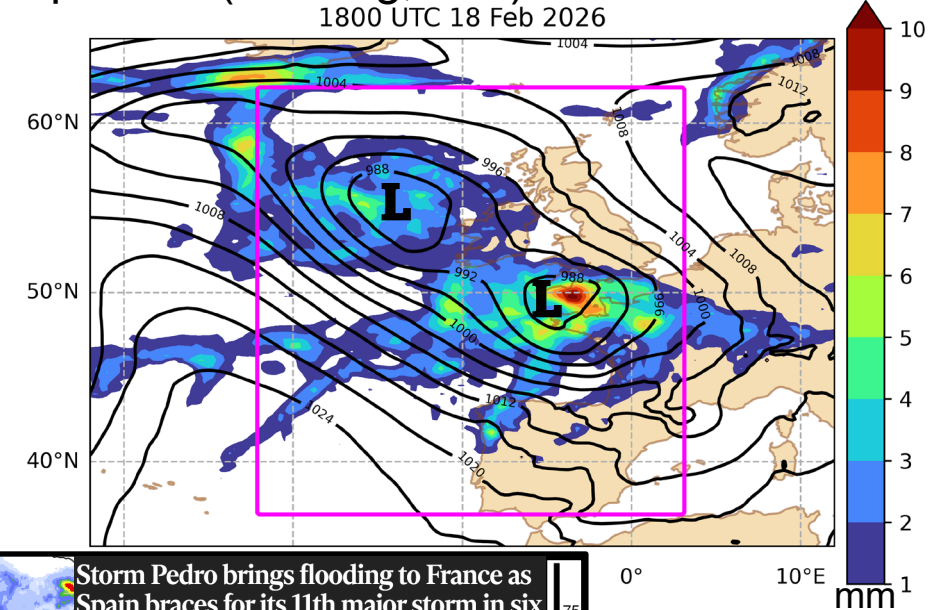
- Where do changes in the initial conditions most strongly affect high impact weather (HIW) forecasts?
  - Observation targeting & system design, dynamics, predictability
- Adjoint sensitivity (Errico 1997; Rabier et al. 1996; Doyle et al. 2019)
  - Quantifies sensitivity of a forecast metric to initial conditions
  - Limitations: computational cost, complex code, short lead time
- ML models are ideal for sensitivity computations
  - Derivatives computed analytically via backpropagation
  - Enables long-lead sensitivities (>2 weeks) (e.g., Vonich & Hakim, 2024)
  - Agree with adjoints for ~48-h integrations (Baño-Medina et al. 2025); correlation of 0.7+ for > 100 cases between ML & NWP adjoints
- Goal: Use ML sensitivity analysis to identify HIW predictability barriers during AR-Recon, NURTURE, NAWDIC, & GARRP
  - 5-day forecast sensitivities using GraphCast (Lam et al. 2023)
  - Case study: Storm Pedro (2026)
  - Establish interpretability

- GraphCast (1° version) used to compute 5-day sensitivities and optimal perturbations
- Loss function
  - Mean Squared Error vs ERA-5 reanalysis
  - 3D temperature, humidity, winds, geopotential, MSLP, 2-m temp., 10-m wind speed, precipitation
  - Computed over W. Europe & E. Atlantic
- Optimal perturbations
  - Iteratively apply sensitivity gradients to initial conditions (captures nonlinearities)

$$x_0^{i+1} = x_0^i - \eta \left( \frac{\partial L}{\partial x_0} \right)^i$$

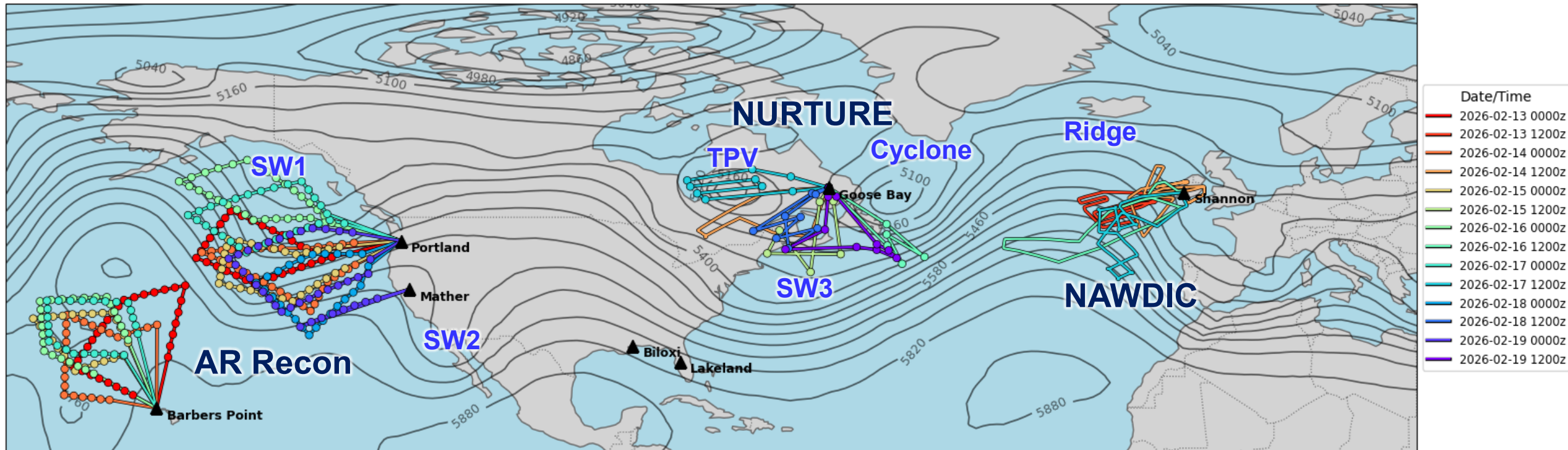
- Storm Pedro (17-20 Feb. 2026)
  - Flooding in France (100-200 mm); UK impacts
  - Wind gusts to 36 m s<sup>-1</sup> (81 mph) in Spain
  - Occurred during AR-Recon, NAWDIC, NURTURE

Sea level pressure (black, hPa) and 6-h accumulated precipitation (shading, mm) from ERA5



# Flight Tracks during Storm Pedro Time Period

AR Recon, NAWDIC, NURTURE Flight Tracks (13-19 Feb. 2026)  
1800 UTC 13 Feb. 500-hPa Geopotential Height Analysis



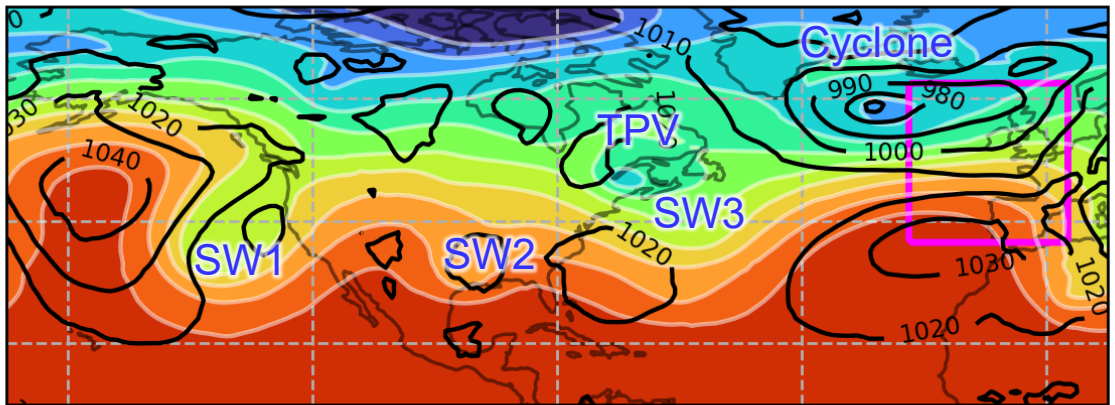
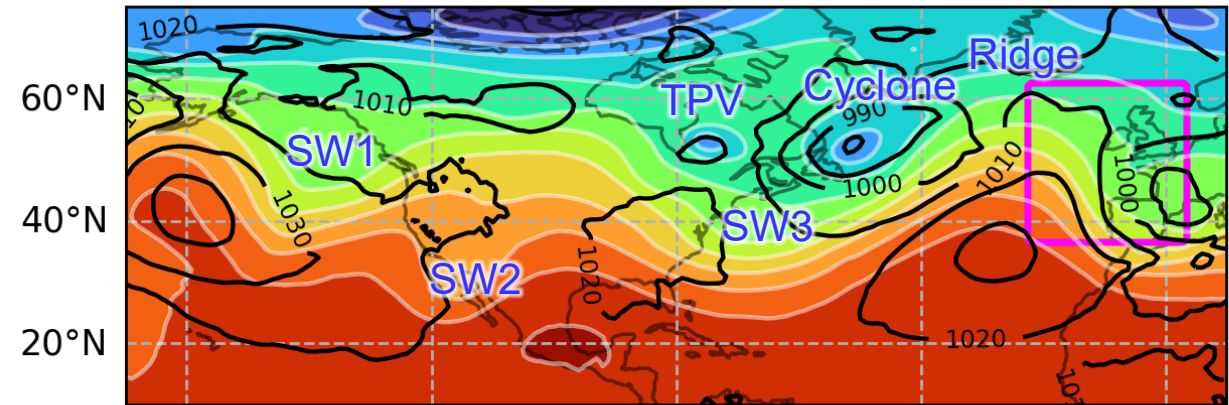
- During 13-19 February, > 20 research flights and many dropsondes deployed
- Excellent case to examine in the context of GARRP goals

# Synoptic Overview

Sea level pressure (black, hPa) and 500-hPa geopotential height (shading, dam) from ERA5

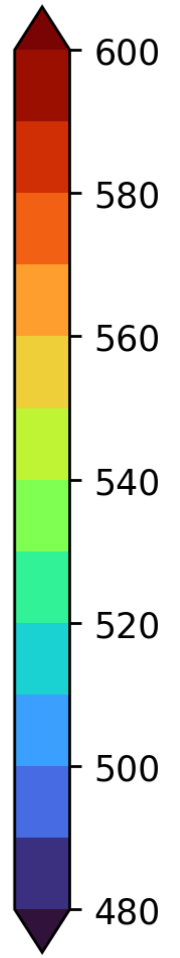
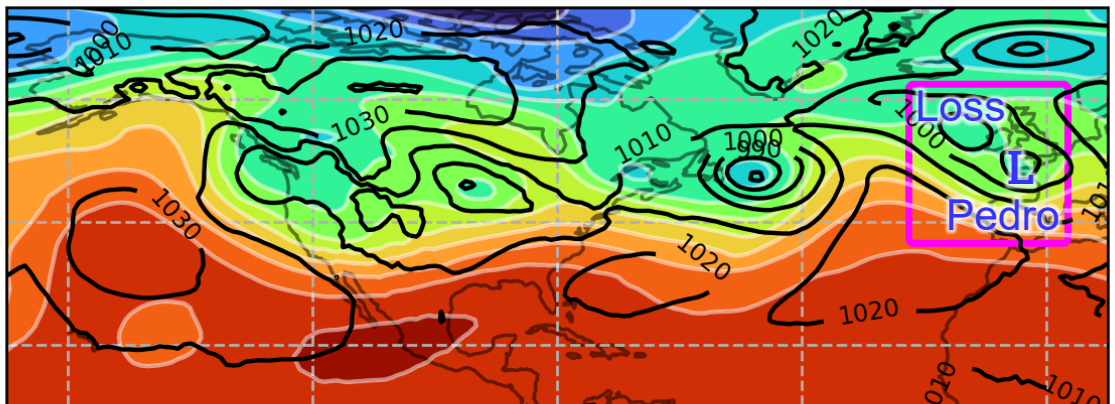
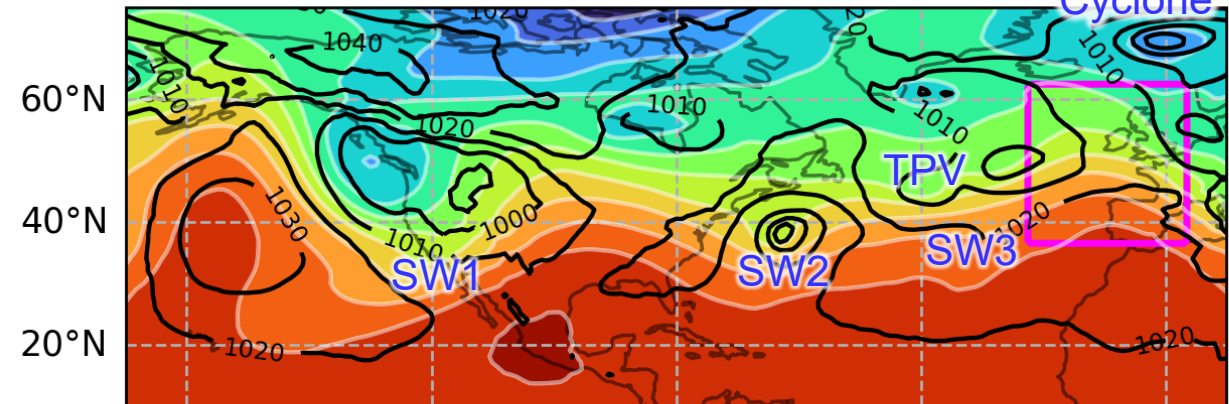
(a) 1800 UTC 13 Feb 2026 ( $t = 0$  h)

(b) 0600 UTC 15 Feb 2026 ( $t = 36$  h)



(c) 0600 UTC 17 Feb 2026 ( $t = 84$  h)

(d) 1800 UTC 18 Feb 2026 ( $t = 120$  h)



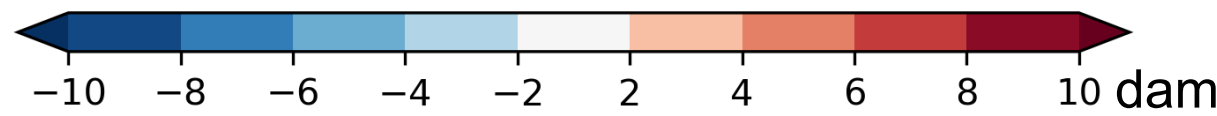
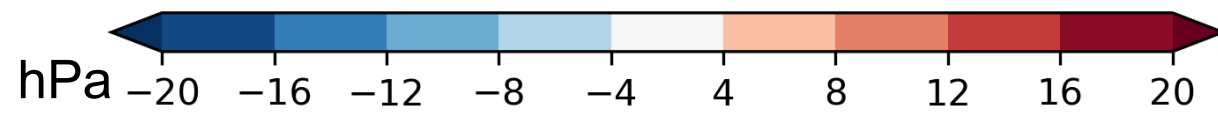
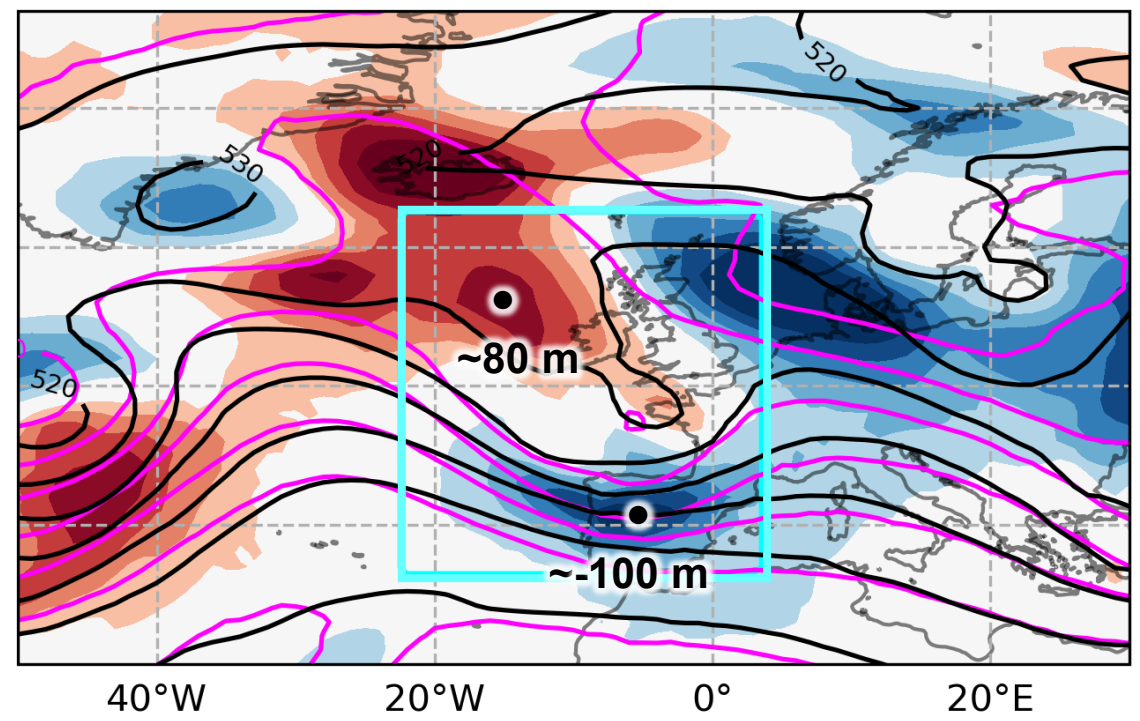
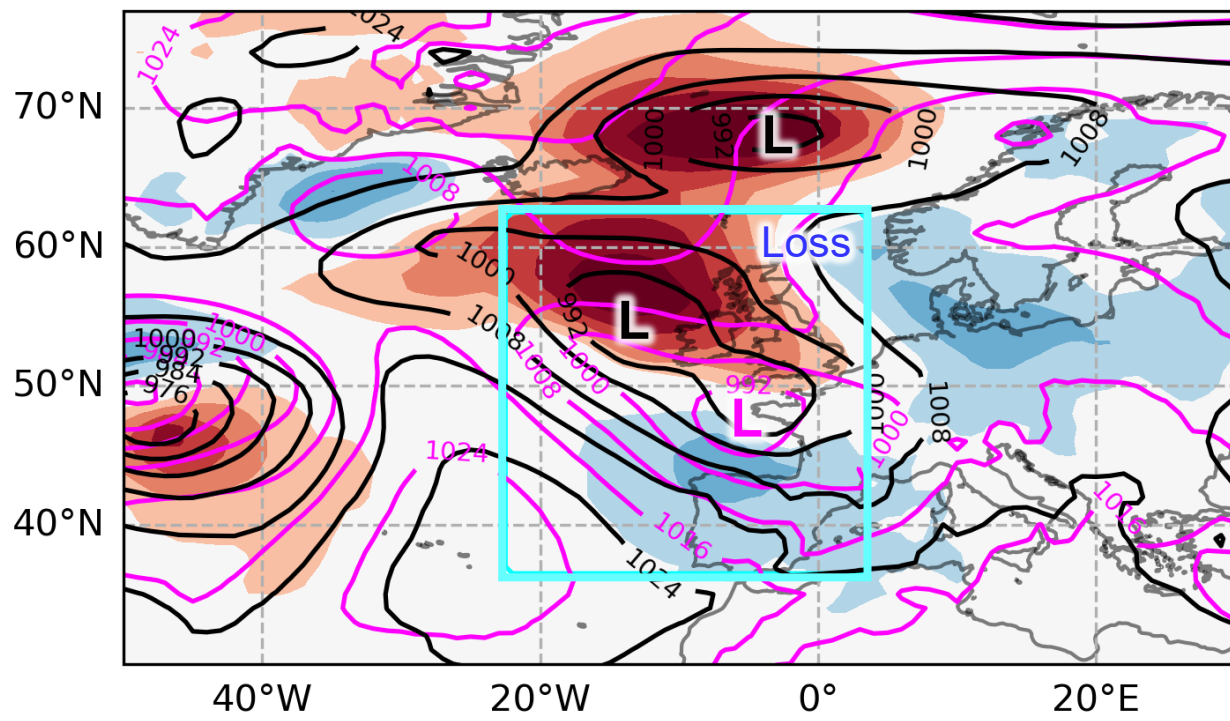
Features impacting predictability: 3 shortwave troughs (SW1-3), East Coast cyclone, ridge, TPV

# GraphCast Forecast Errors

5-day GraphCast Forecast (magenta), ERA5 (black), Forecast minus ERA5 (shading) (1800 UTC 18 Feb)

(a) SLP(hPa)

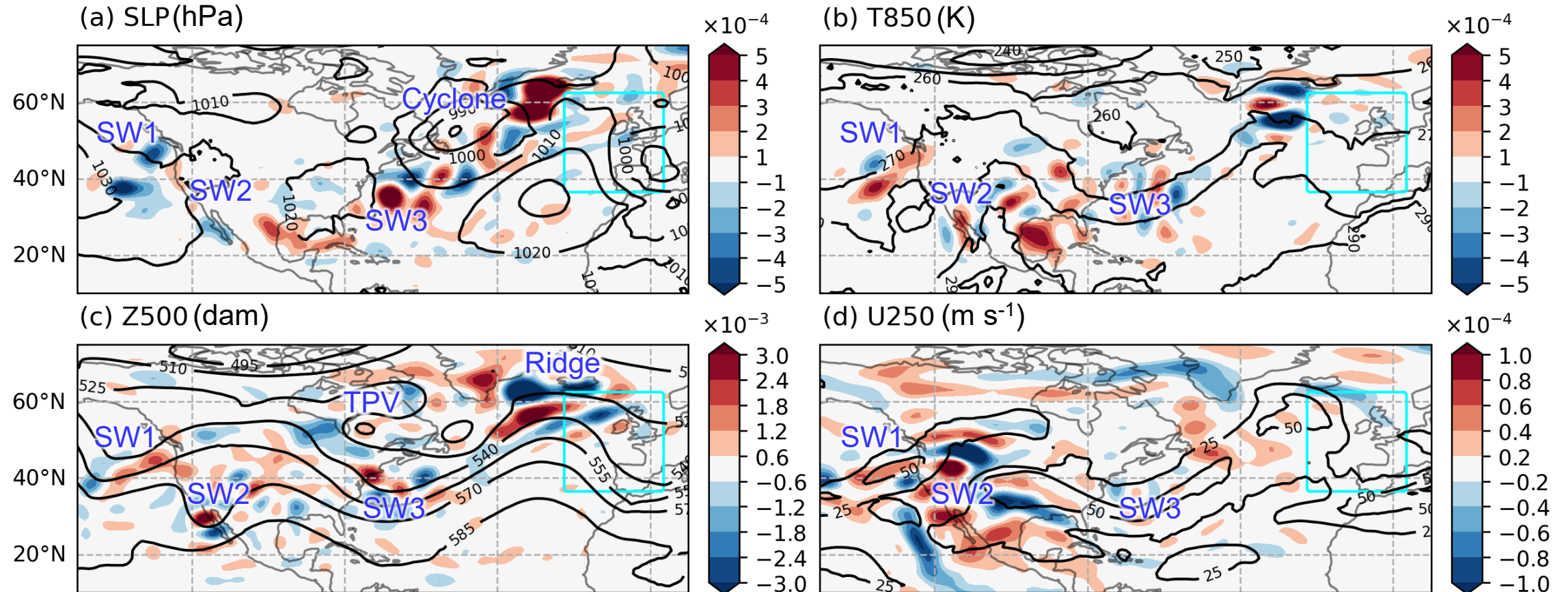
(b) Z500(dam)



Cyan box = region over which loss function (5-day forecast error over all variables and levels) is averaged when computing sensitivity gradients

# Sensitivity of 5-day Forecast Error to Initial Conditions

5-day Sensitivity (shading) and Initial Conditions from ERA5 (black) Valid at 1800 UTC 13 Feb. 2026

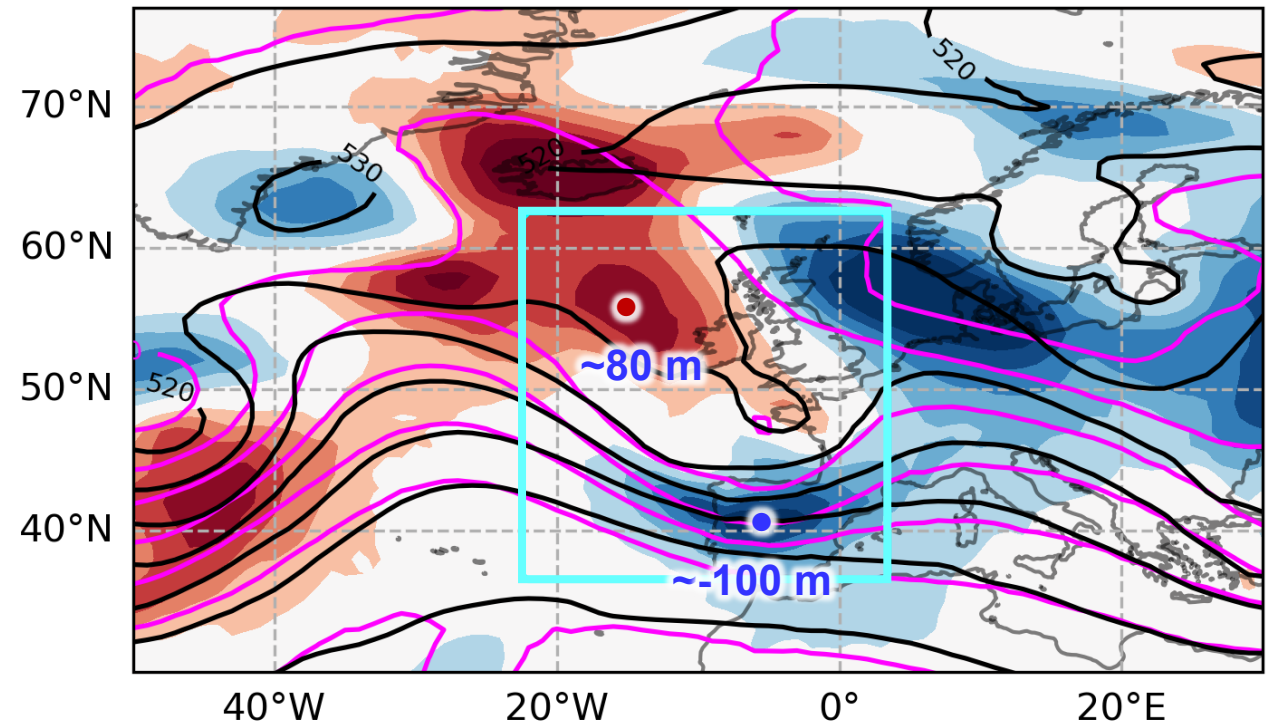


- SLP sensitivity occurs along the Gulf Stream corridor
- Sensitivities are tilted upstream with altitude similar to adjoints [tilted against the mean shear to maximize transient response (e.g. Orr 1907; Rabier et al. 1996)]

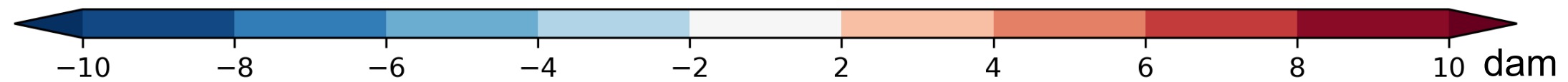
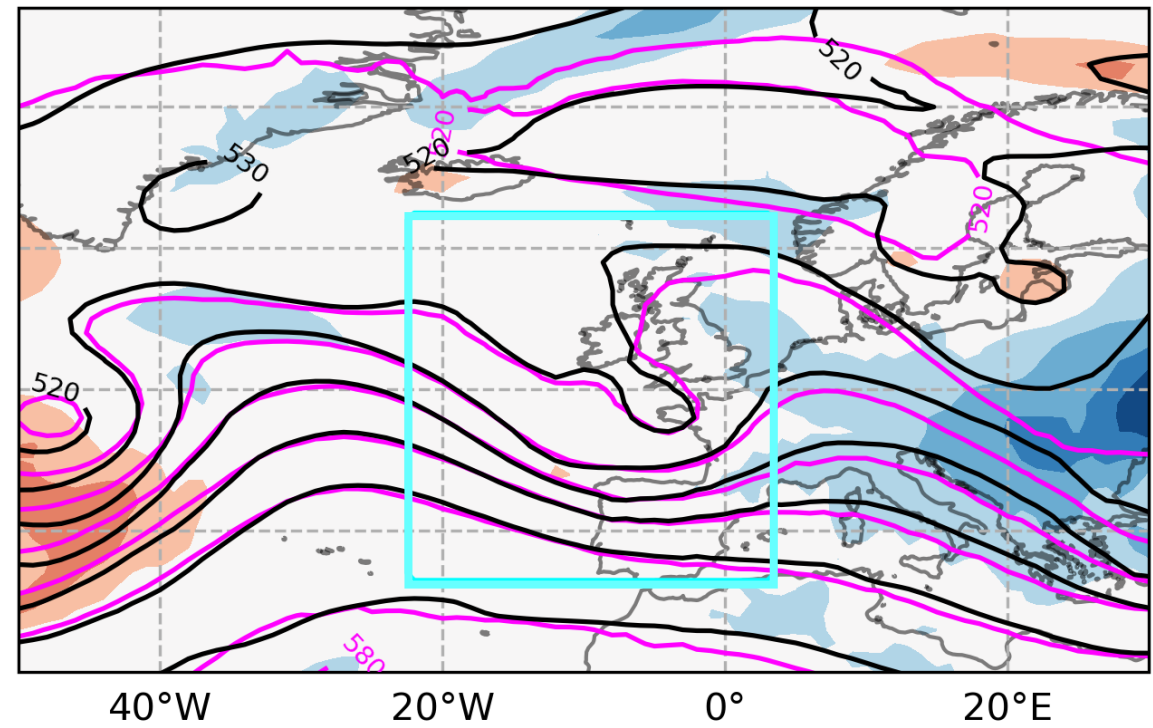
# Optimal Perturbations

5-day GraphCast forecast (magenta), ERA5 (black), and Forecast minus ERA5 (shading) for 500-hPa geopotential height (dam) valid at 1800 UTC 18 Feb 2026

(a) Original



(b) Optimized

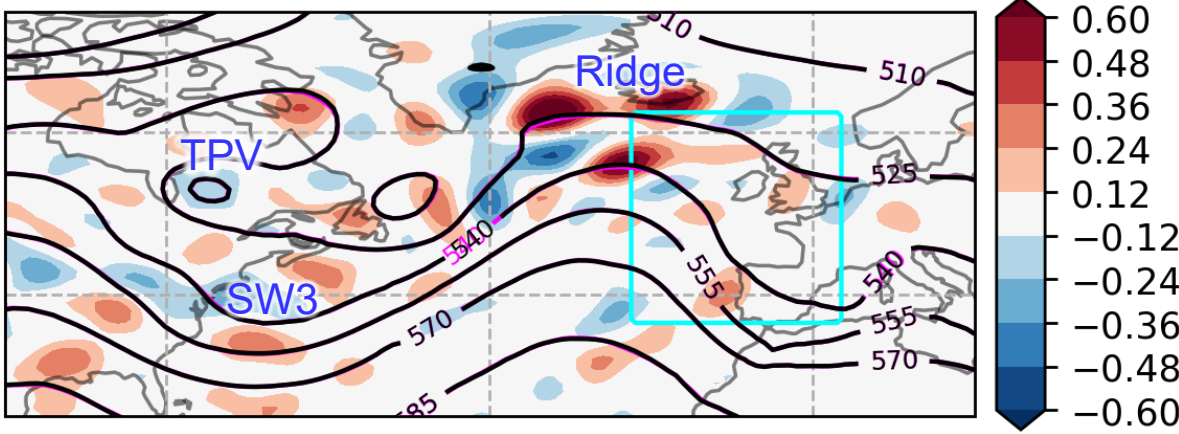


Optimal perturbations are extremely impactful in and around the loss region

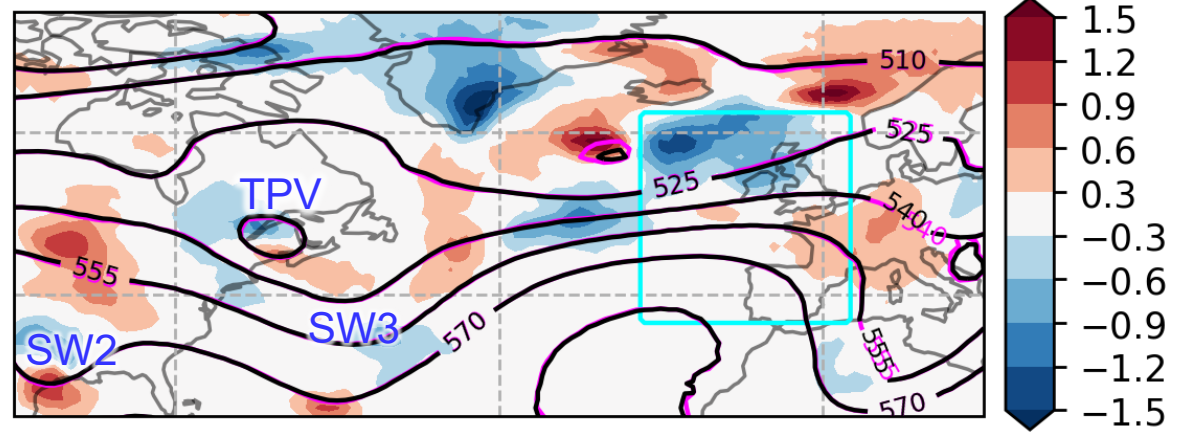
# Z500 Perturbation Evolution

Original forecast (magenta), Optimal forecast (black), and Optimal minus Original (shading) (dam)

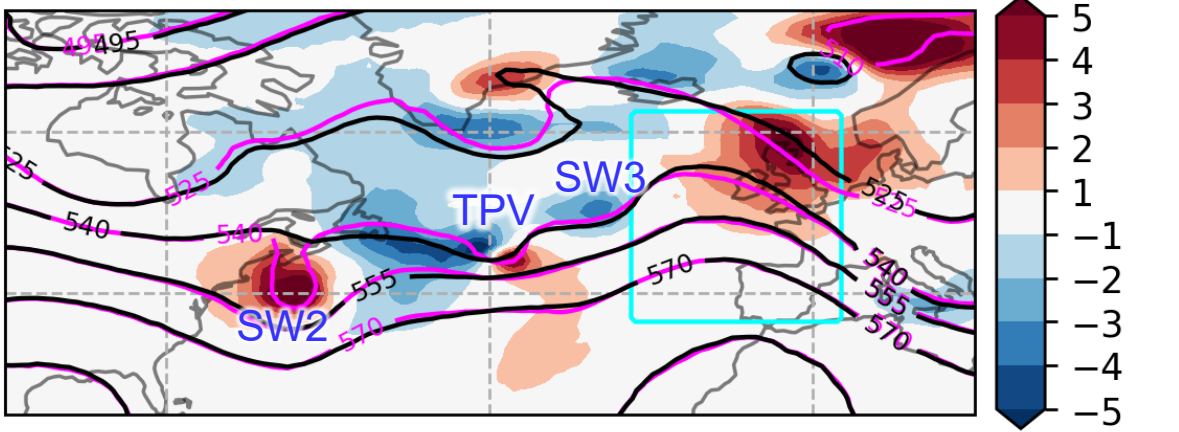
(a) 1800 UTC 13 Feb 2026 ( $t = 0$  h) (dam)



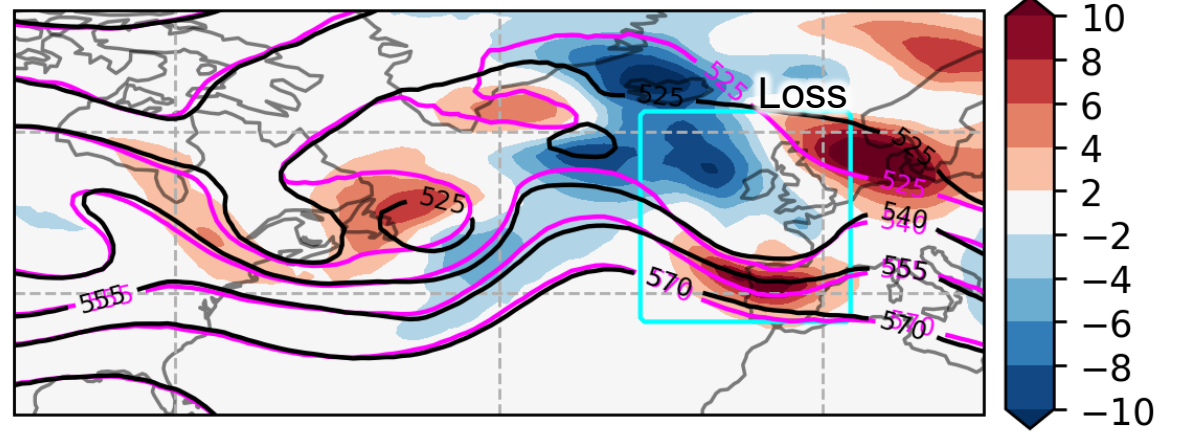
(b) 0600 UTC 15 Feb 2026 ( $t = 36$  h) (dam)



(c) 0600 UTC 17 Feb 2026 ( $t = 84$  h) (dam)



(d) 1800 UTC 18 Feb 2026 ( $t = 120$  h) (dam)

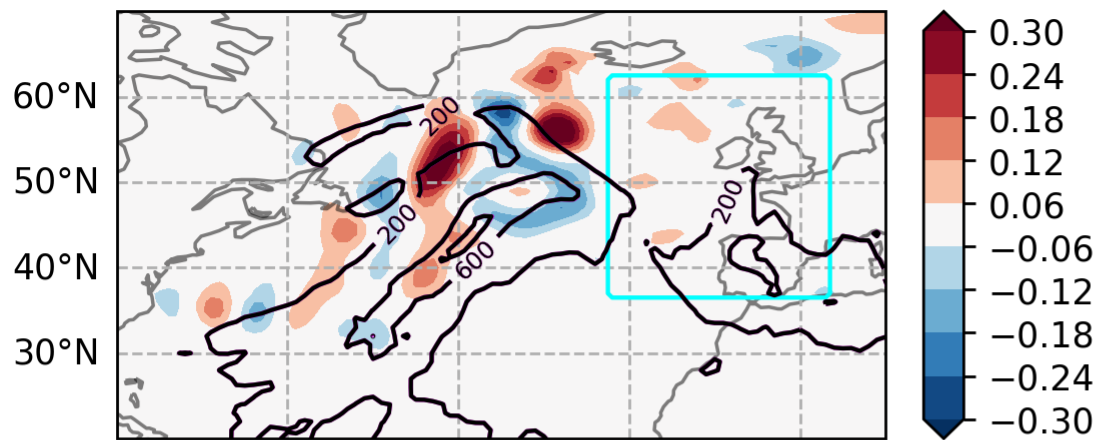


Largest initial perturbations are near the ridge, followed by rapid growth in the waveguide and SW2 & 3 consistent with Rossby wave packet dynamics and non-normal growth (Farrell 1989)

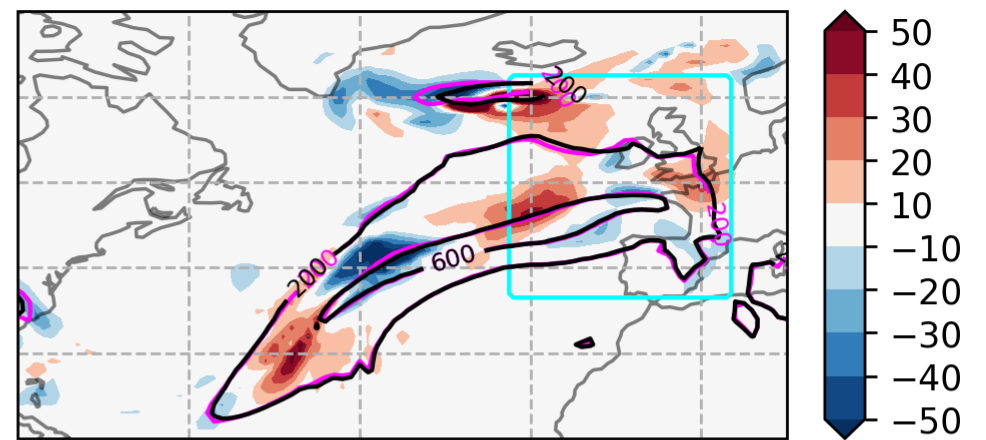
# IVT Perturbation Evolution

Original forecast (magenta), Optimal Forecast (black), and Optimal minus Original (shading)

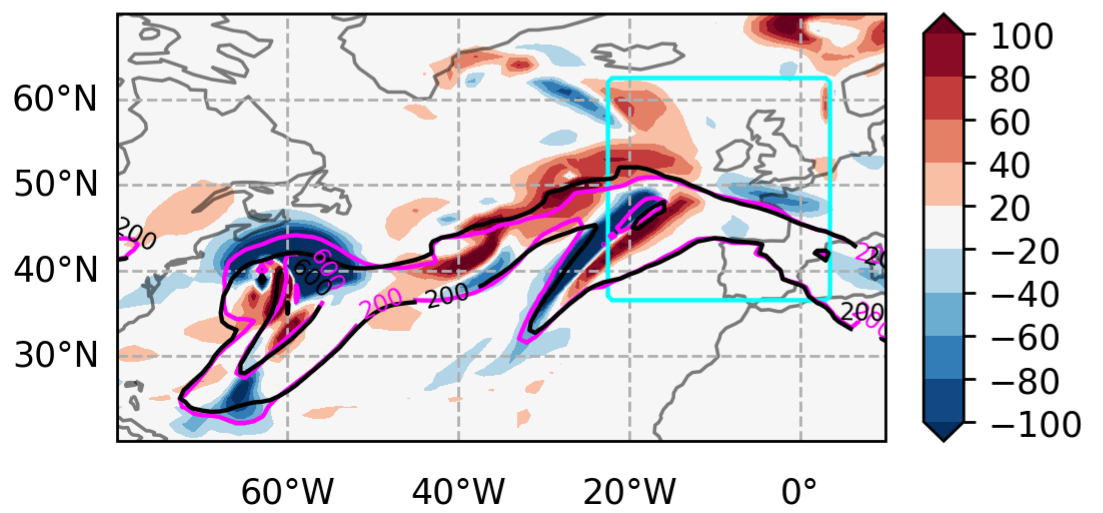
(a) 1800 UTC 13 Feb 2026 ( $t = 0$  h)



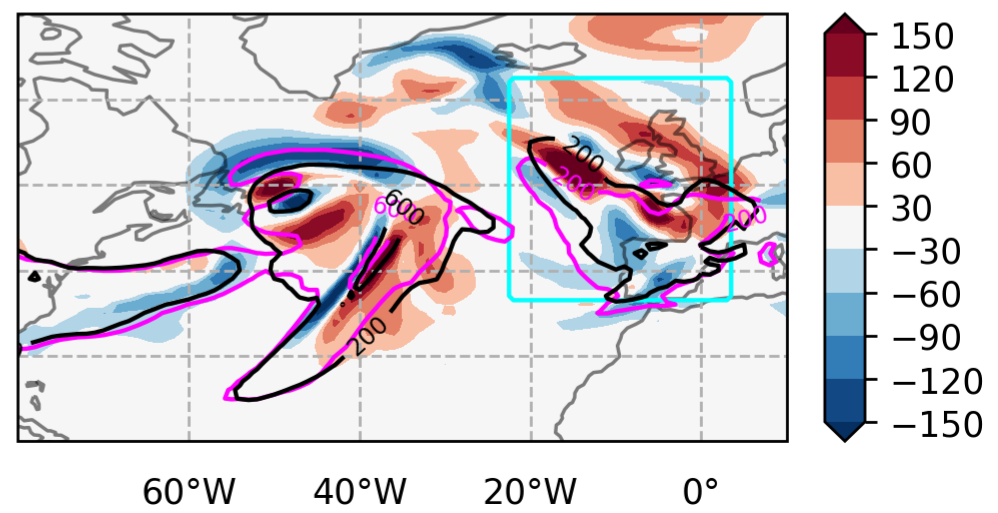
(b) 0600 UTC 15 Feb 2026 ( $t = 36$  h)



(c) 0600 UTC 17 Feb 2026 ( $t = 84$  h)



(d) 1800 UTC 18 Feb 2026 ( $t = 120$  h)

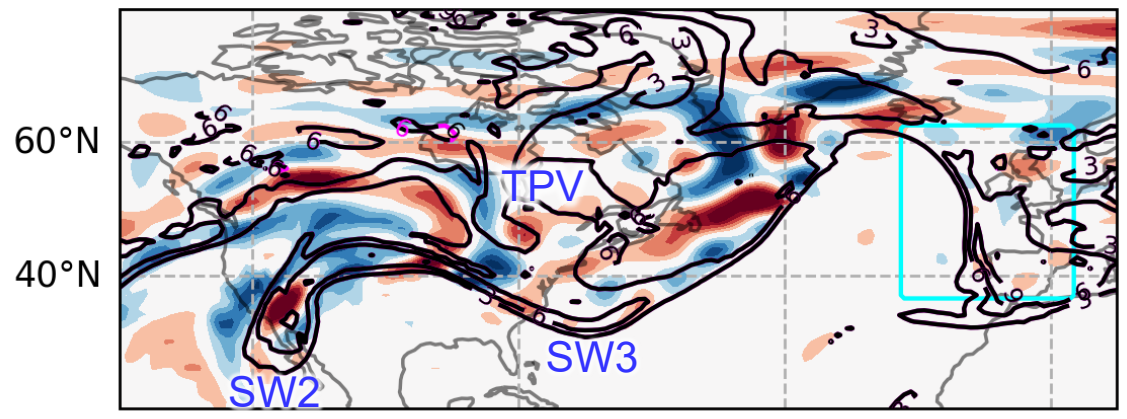


Initially small IVT perturbations grow rapidly and intensifies the AR near Europe at final time

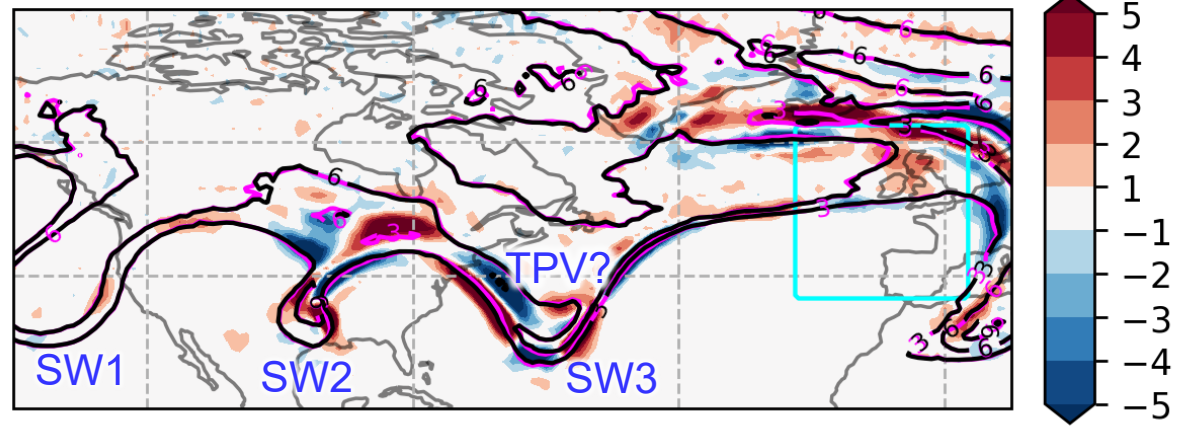
# 250-hPa PV Evolution

Original forecast (magenta), Optimal Forecast (black), and Optimal minus Original (shading)

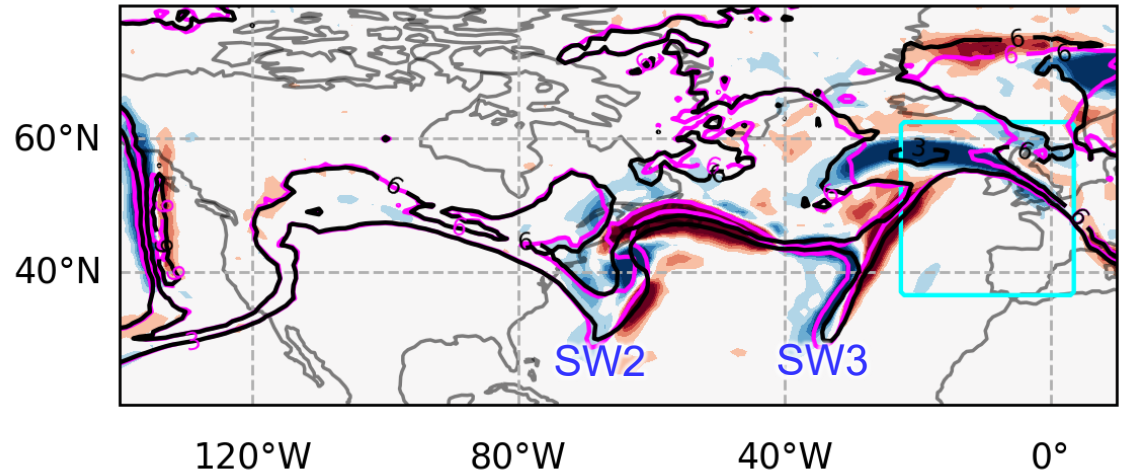
(a) 1800 UTC 13 Feb 2026 ( $t = 0$  h)



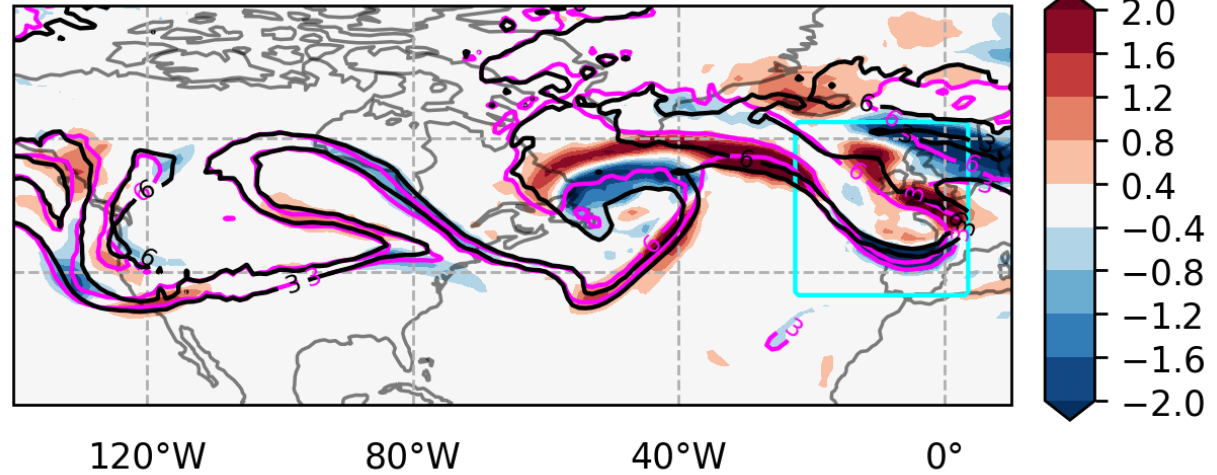
(b) 0600 UTC 15 Feb 2026 ( $t = 36$  h)



(c) 0600 UTC 17 Feb 2026 ( $t = 84$  h)






(d) 1800 UTC 18 Feb 2026 ( $t = 120$  h)

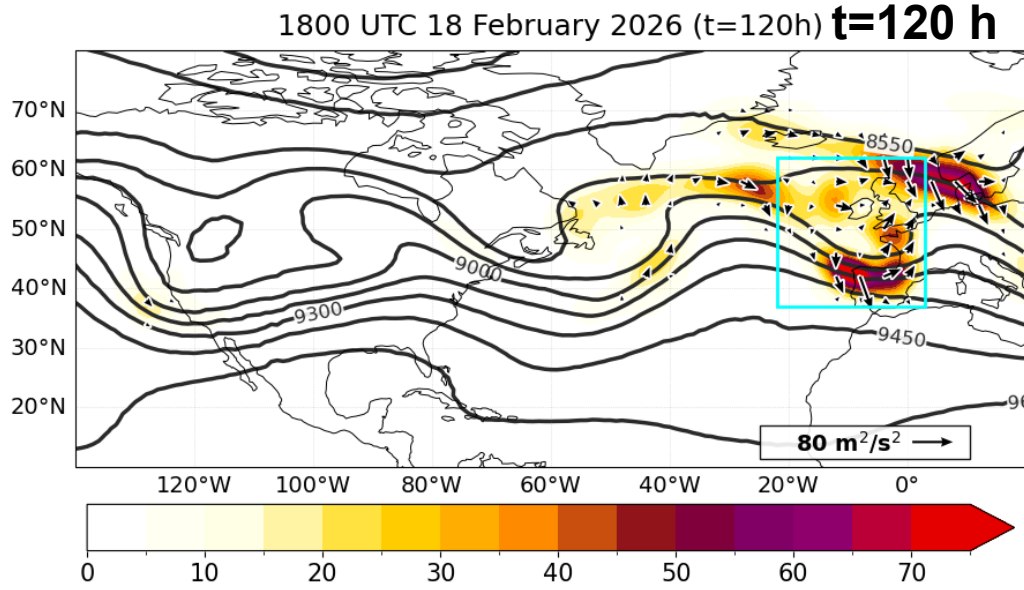
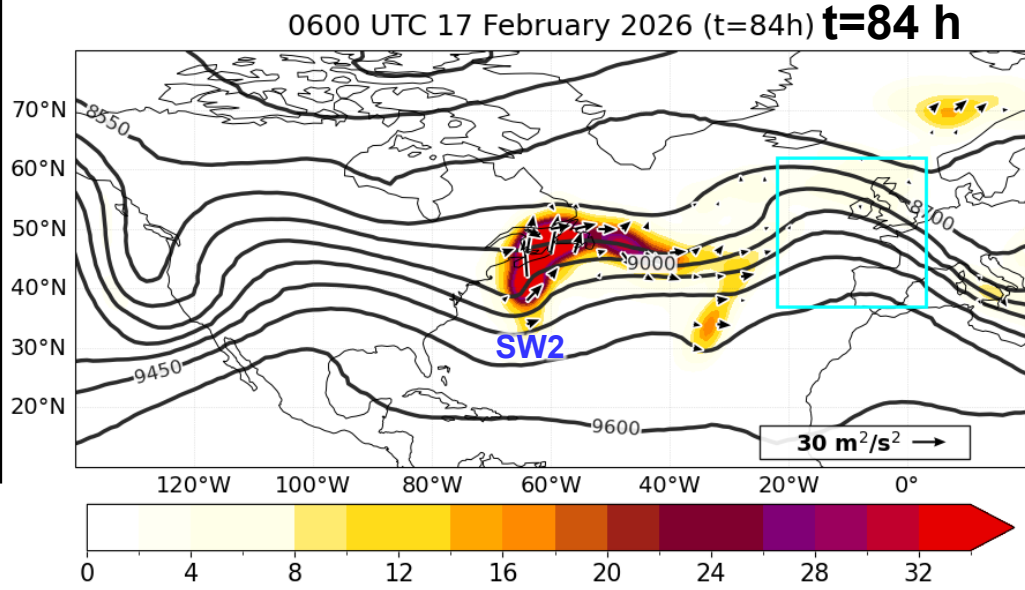
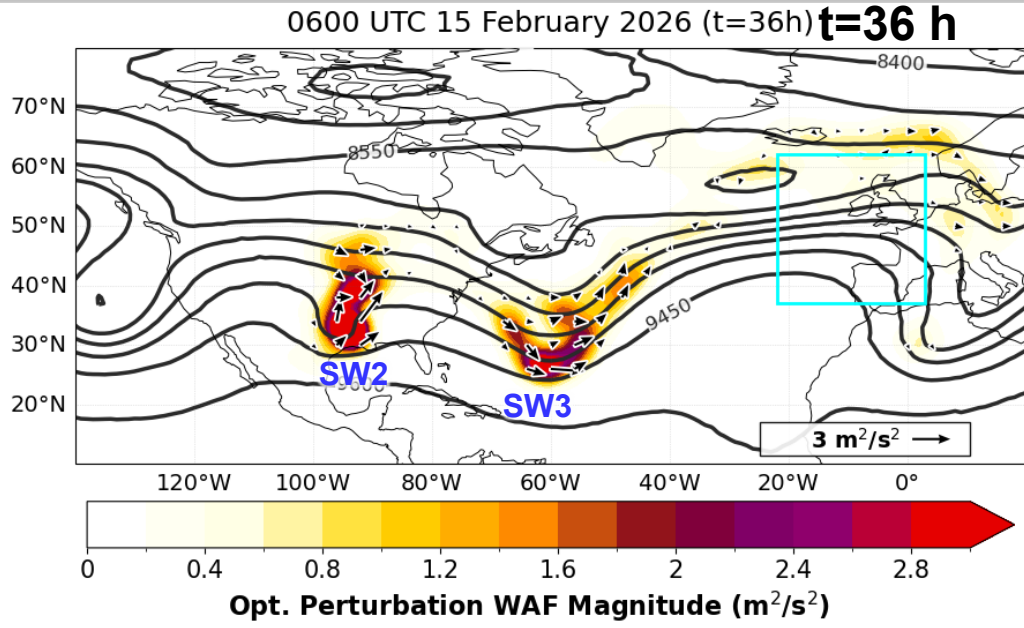
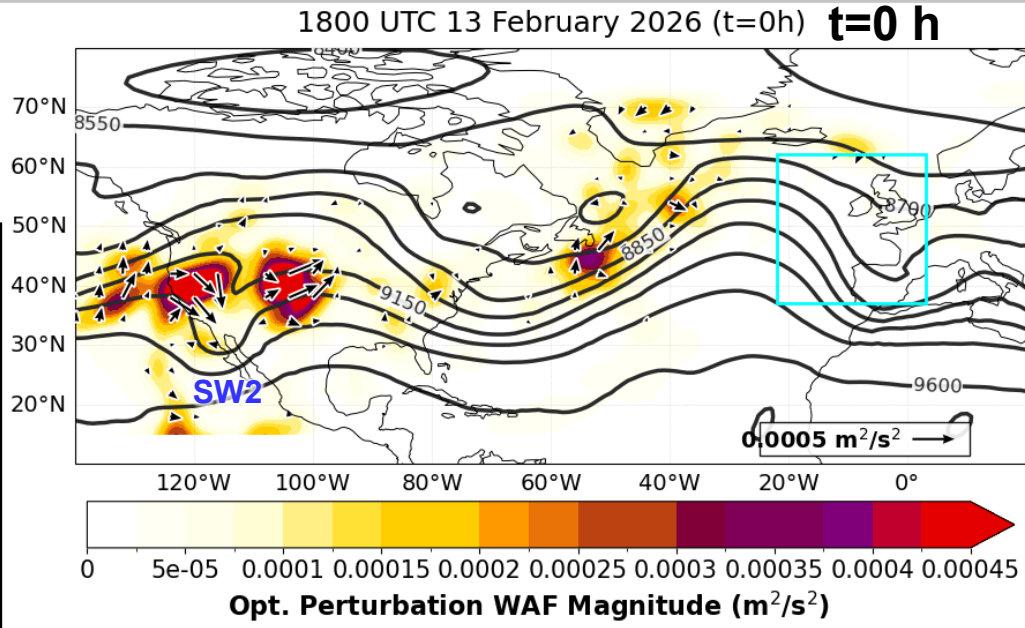


PV optimal perturbations grow rapidly and propagate along the waveguide and sloping tropopause

# Optimal Perturbation Wave Activity Flux (WAF)

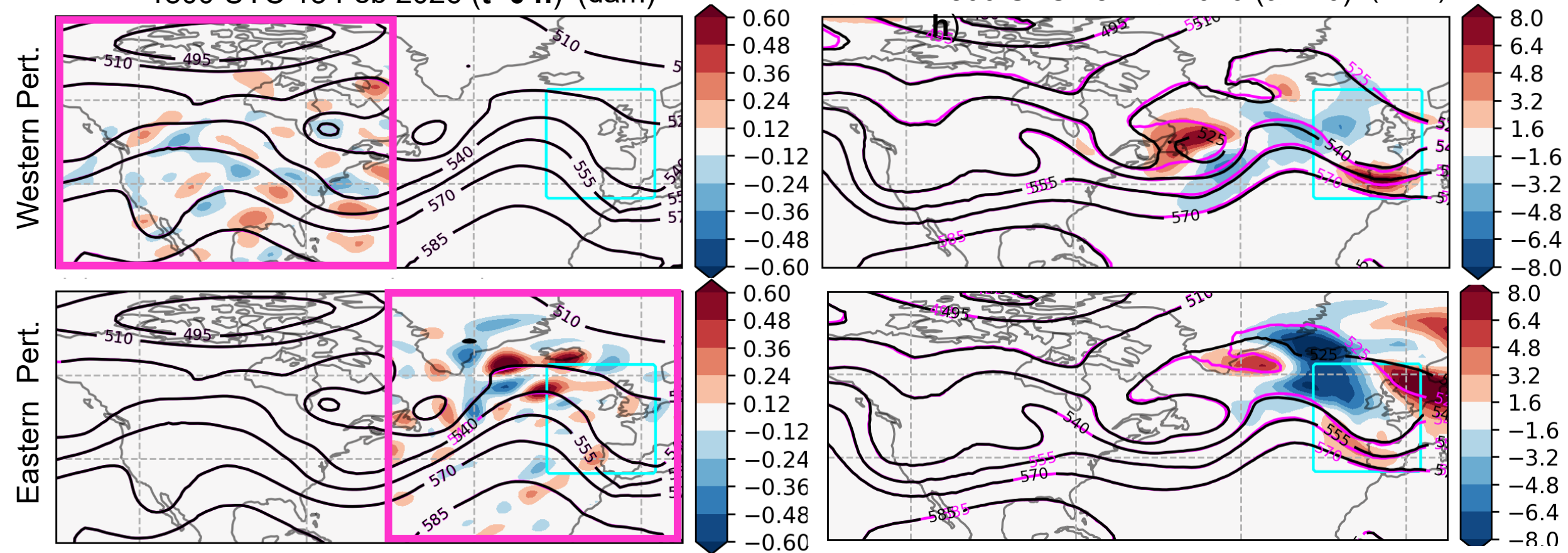
300-hPa heights ———  
 Pert. WAF magnitude   
 Pert. WAF vectors   
 Forecast WAF mag. 

- Wave activity flux (WAF) (Takaya-Nakamura 2001) identifies Rossby wave packets & propagation direction
- Perturbation WAF acts to reinforce background Rossby wave packets, extract energy from background flow, and disperse energy downstream



# Eastern vs. Western Z500 Perturbations

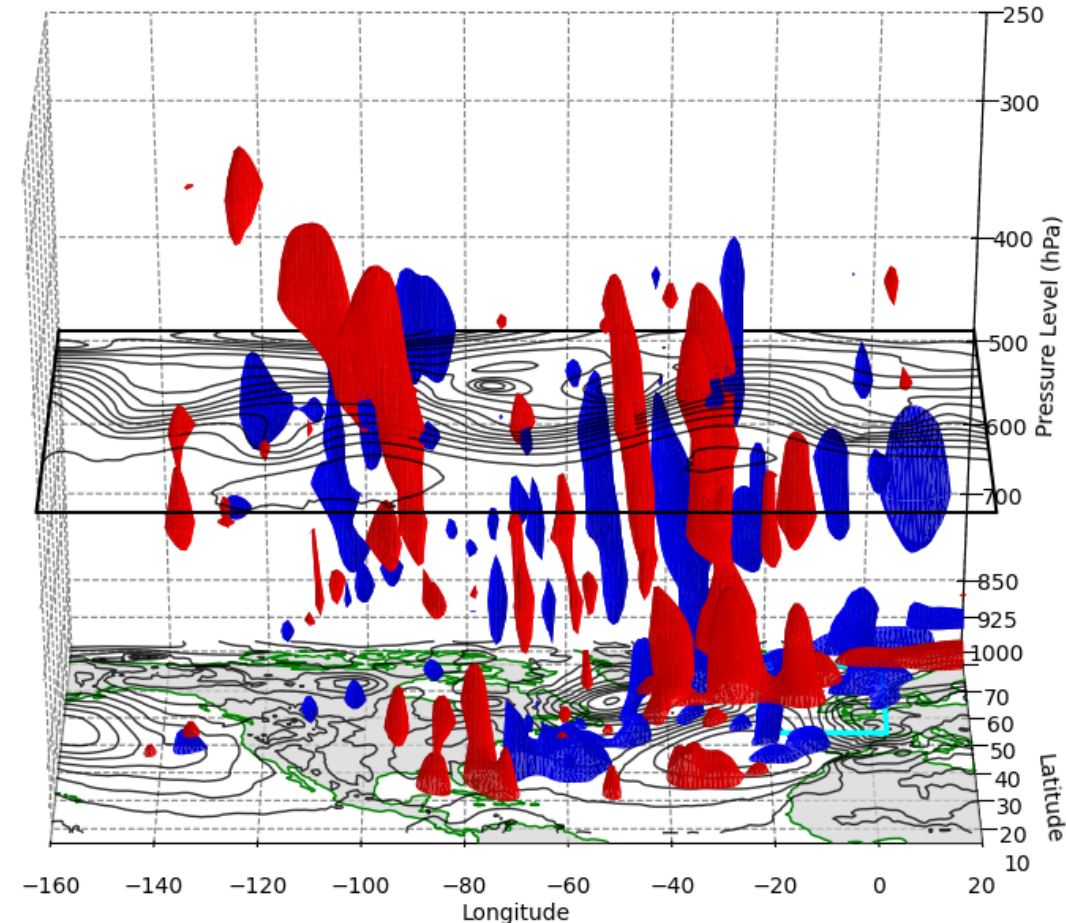
Z500 Perturbations (dam); forecast (magenta), perturbed (black), and perturbed minus original (shading)  
 1800 UTC 13 Feb 2026 (t=0 h) (dam)      1800 UTC 18 Feb 2026 (t=120) (dam)



- Separating perturbations by region provides insight into the error sources and transient growth
- Western perturbations propagate and grow rapidly, impacting the jet, ARs, & downstream trough
- Eastern perturbations propagate and grow slower, modifying downstream flow north of the jet

- GraphCast sensitivity gradients are dynamically-consistent and valid to ~10+ days, not possible using NWP adjoints
- Optimal perturbations grow rapidly, amplify along the jet and drive large 5-day forecast errors in downstream HIW
- Upstream error sources (troughs, ARs, and TPVs) limit predictability through Rossby wave dispersion along the jet
- ML sensitivity analysis identifies error sources, informs adaptive observations (AR Recon, NURTURE, GARRP), and advances understanding of HIW predictability
- Future:
  - ML sensitivities to NURTURE, AR Recon, GARRP to understand what limits HIW predictability
  - Linking ML Models/Sensitivity, Direct Obs. Prediction, autonomous observing systems to improve predictions

3D View (t=0): Surface SLP, 500 hPa Heights & Temp Pert. Isosurfaces  
500hPa: Contoured Geopotential  
3D Volume: Temp Pert. (Red: +0.018, Blue: -0.018)

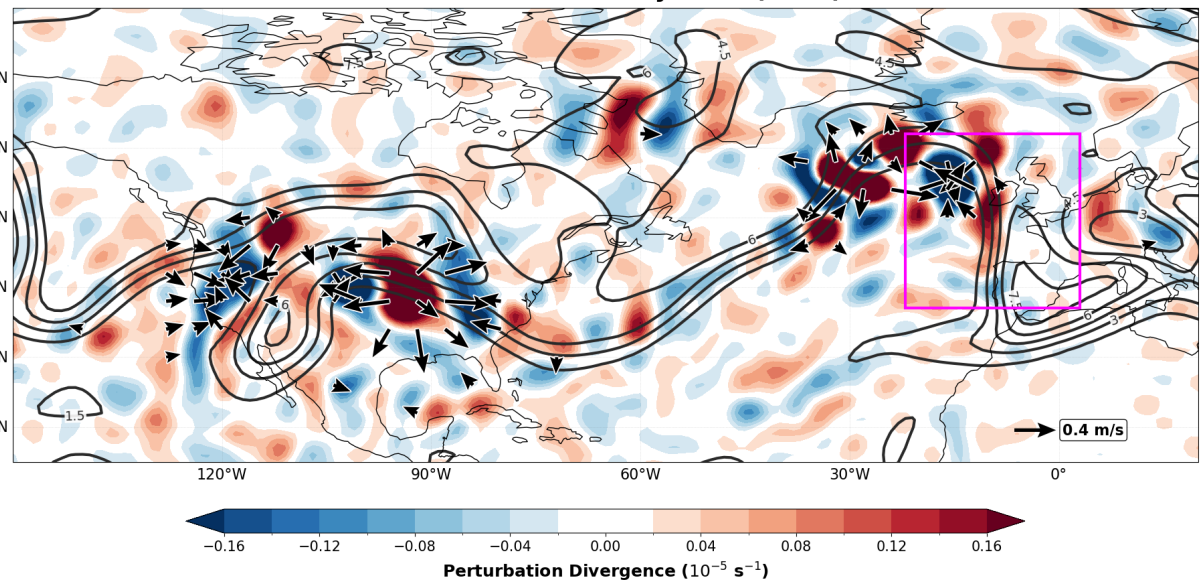


# Extra Slides

# 250-hPa Rossby Wave Forcing

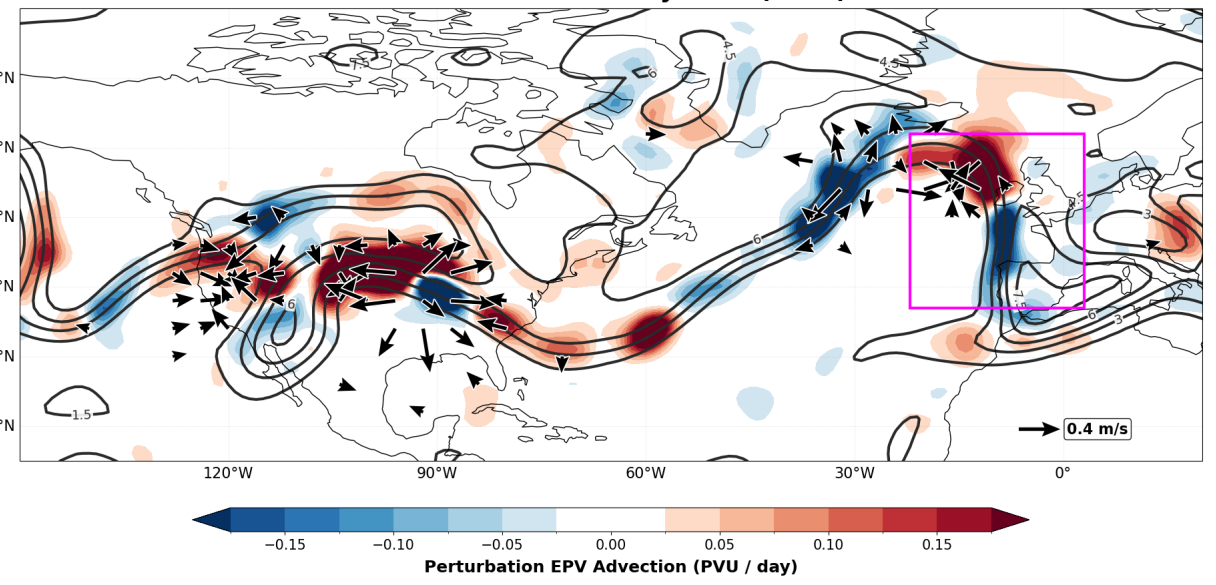
250-hPa Perturbation Divergence (shading); PV (contours),  
Perturbation Irrotational Wind Vectors (6 h)

0000 UTC 14 February 2026 (t=6h)



PV Advection by Perturbation Irrotational Wind (shading)  
PV (contours); Perturbation Irrotational Wind Vectors (6h)

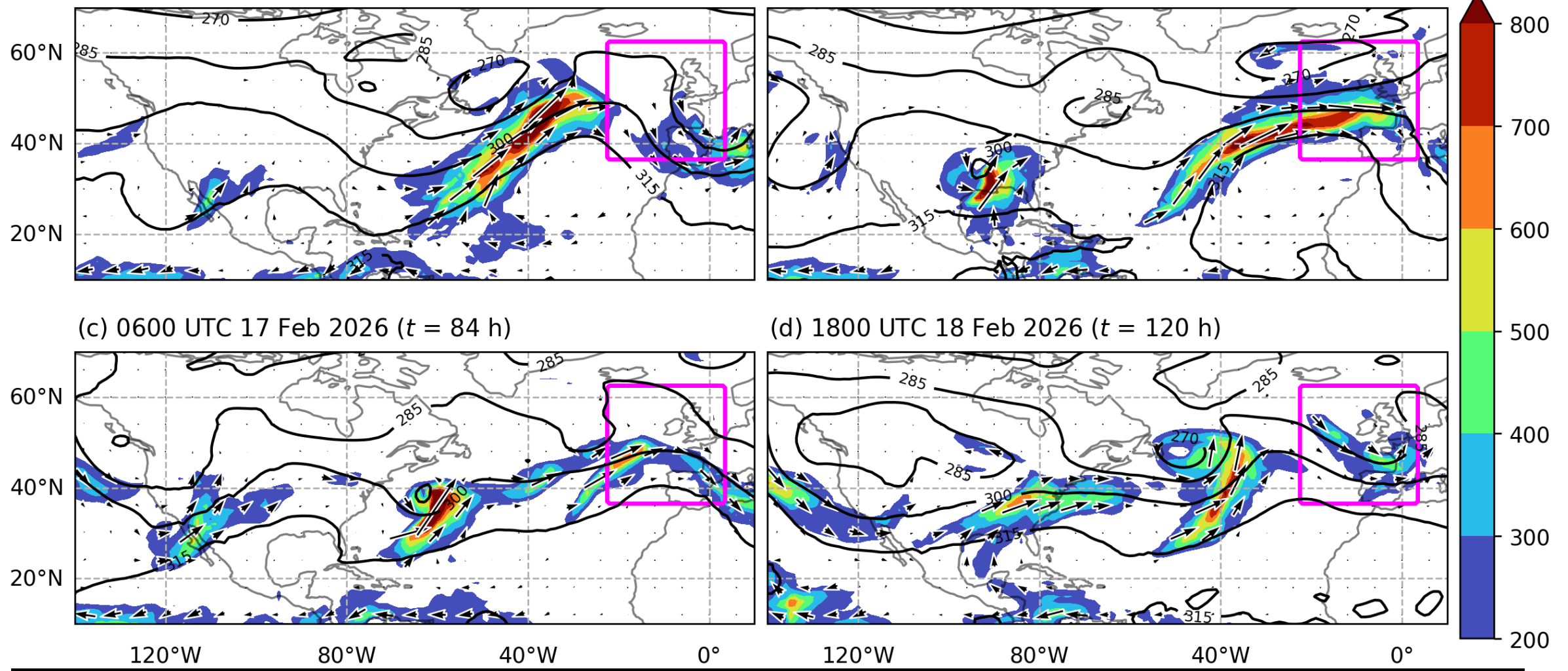
0000 UTC 14 February 2026 (t=6h)



- Optimal perturbations increase divergent outflow early in forecast, especially near SW2 and cyclone
- Strong advection of PV by the perturbation irrotational wind near SW2

# Synoptic Overview

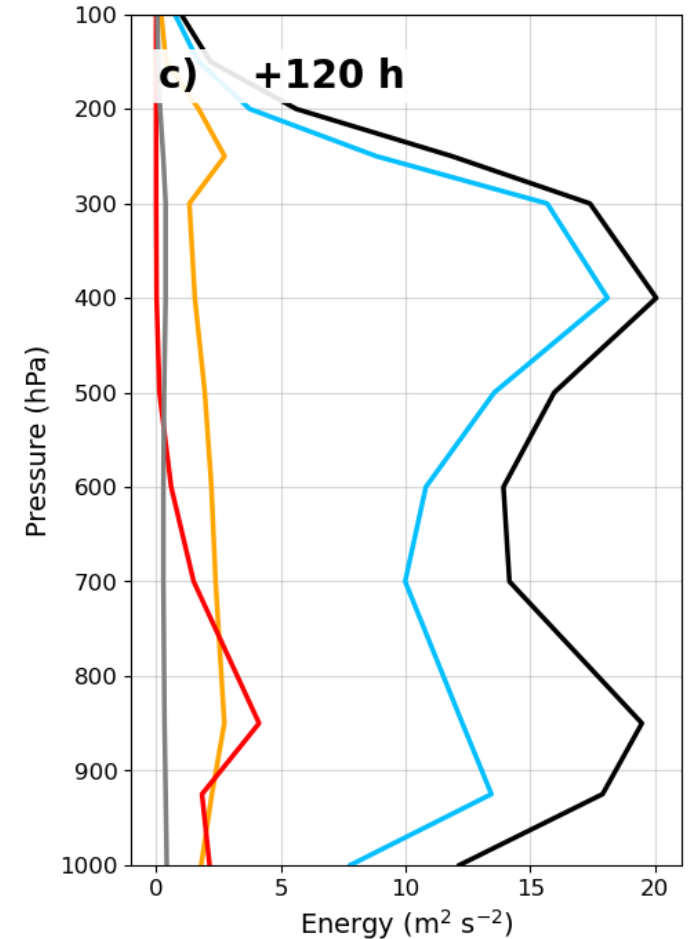
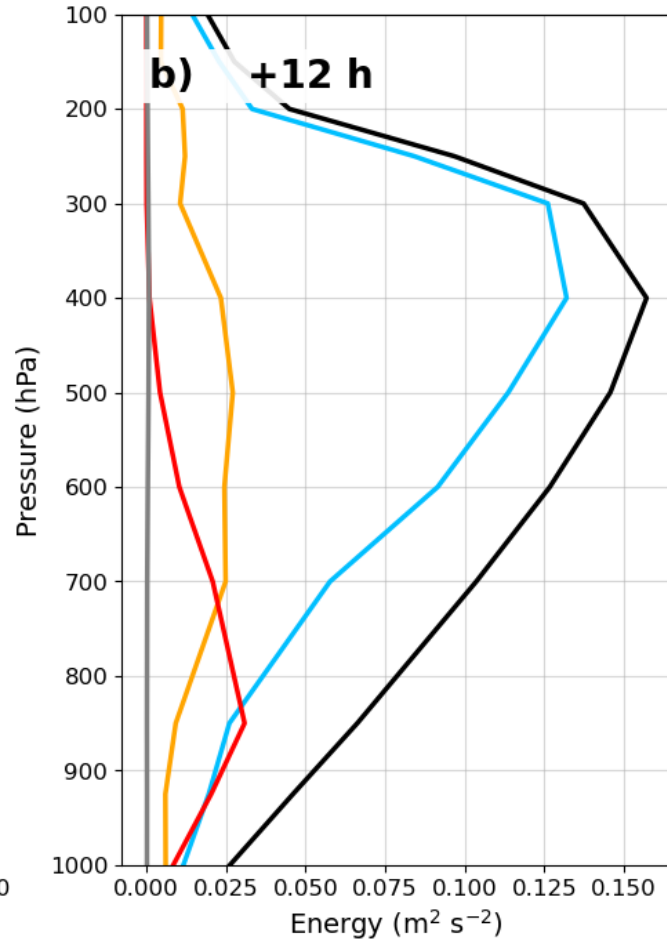
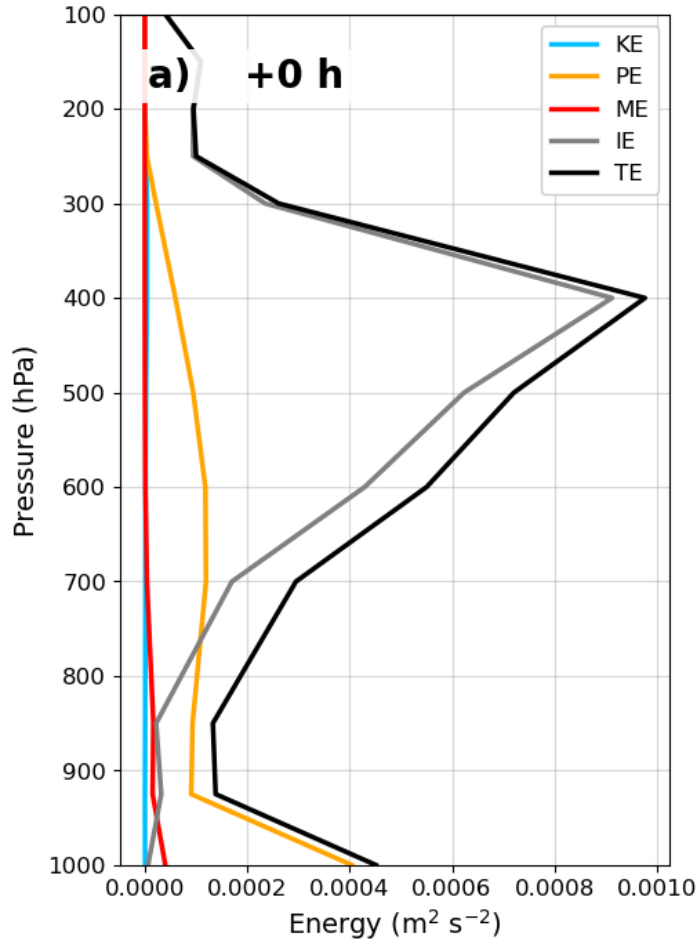
IVT Vectors and Magnitude (shading,  $\text{kg m}^{-1} \text{s}^{-1}$ ) and 700-hPa Geopotential Height (black, dam)  
 (a) 1800 UTC 13 Feb 2026 ( $t = 0 \text{ h}$ )      (b) 0600 UTC 15 Feb 2026 ( $t = 36 \text{ h}$ )



Atmospheric rivers were present in the East, Central, West Atlantic during the forecast

# Optimal Perturbation Energy Budget

- Rapid conversion of upstream internal energy to downstream kinetic energy (non-normal transient growth)
- Energy conversion rates show that initial growth occurs via baroclinic production that is peaked in mid-levels; PE→KE conversion also contributes later

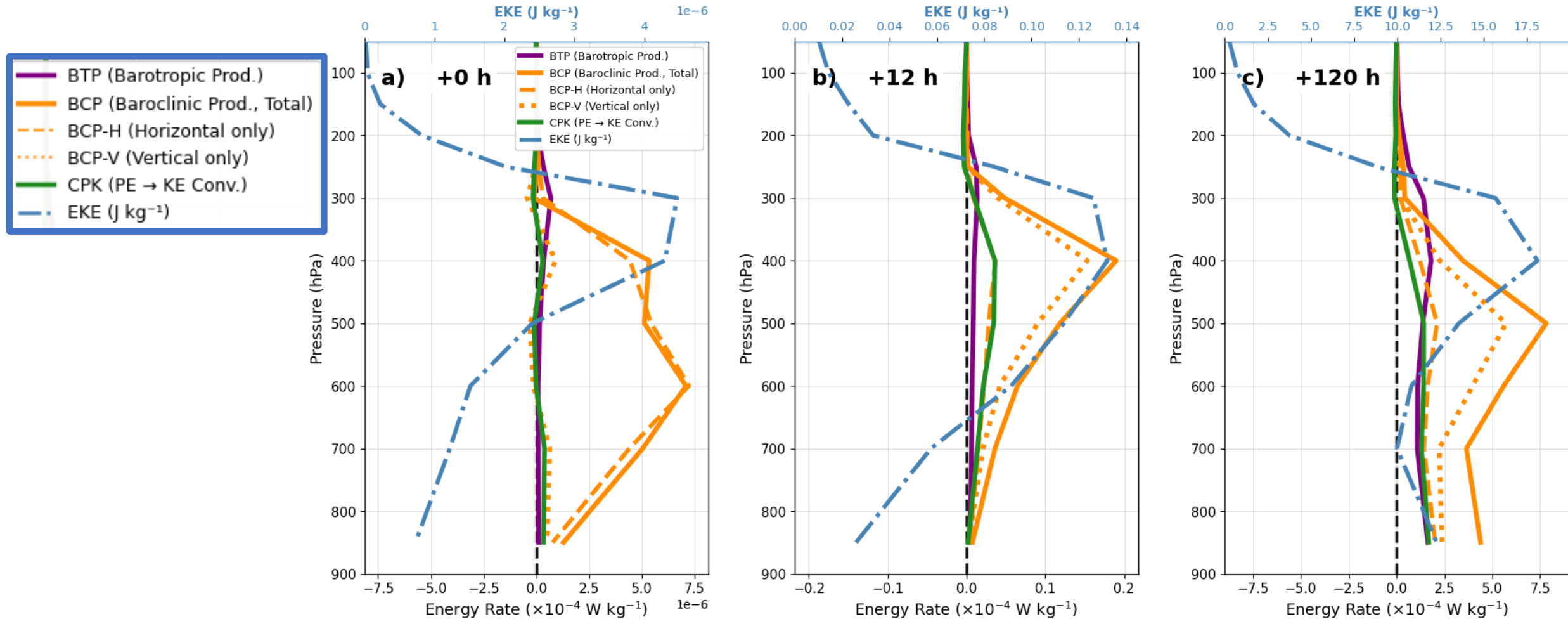


$$E = \frac{1}{2A} \int \left[ \underbrace{(u'^2 + v'^2 + w'^2)}_{\text{KE}} + \underbrace{\frac{C_p}{T_r} T'^2}_{\text{PE}} + \underbrace{\frac{RT_r}{p_{sr}^2} p'^2}_{\text{IE}} + \underbrace{\frac{l_v^2}{C_p T_r} q_v'^2}_{\text{Moist}} \right] dAd\sigma$$

Total
KE
PE
IE
Moist

# Optimal Perturbation Energy Conversion Rates

Init: 2026021318 | Domain: 10°-80°N, -140°-20°E



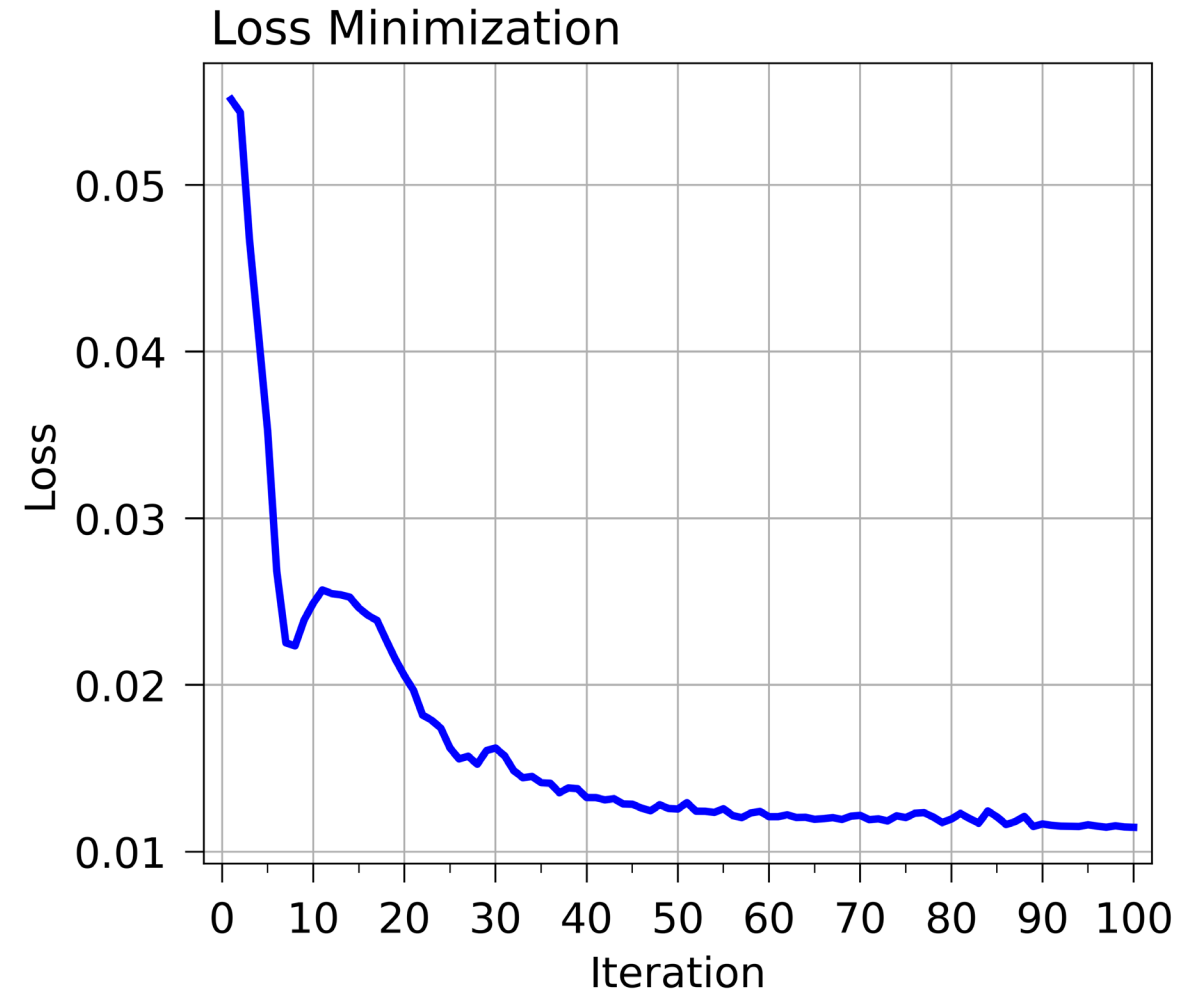
- Diagnosis of optimal perturbation energy conversion rates [e.g., Lorenz (1955); Holton and Hakim (2013)]
- Rapid initial growth via baroclinic production peaked in mid-levels; PE→KE conversion contributes later

# Computing “Optimal” Initial Conditions

- What are the changes (i.e., perturbations) to the initial conditions that will minimize forecast error?
- Obtain by iteratively applying sensitivity gradients to initial conditions

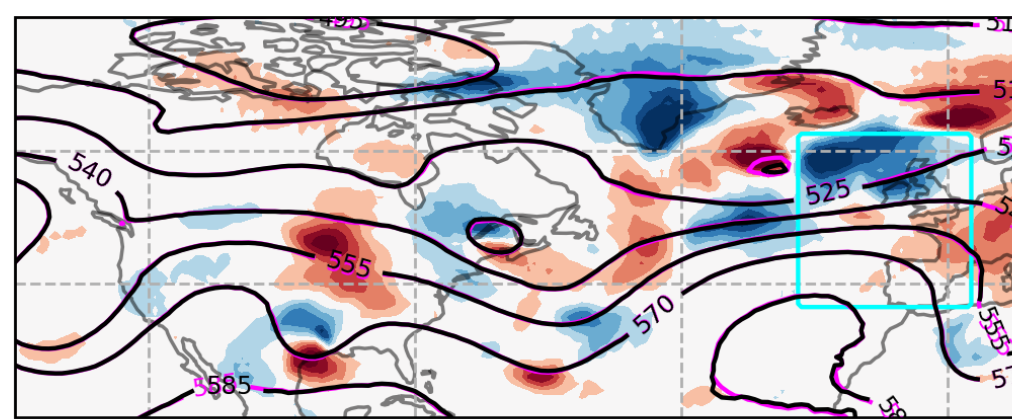
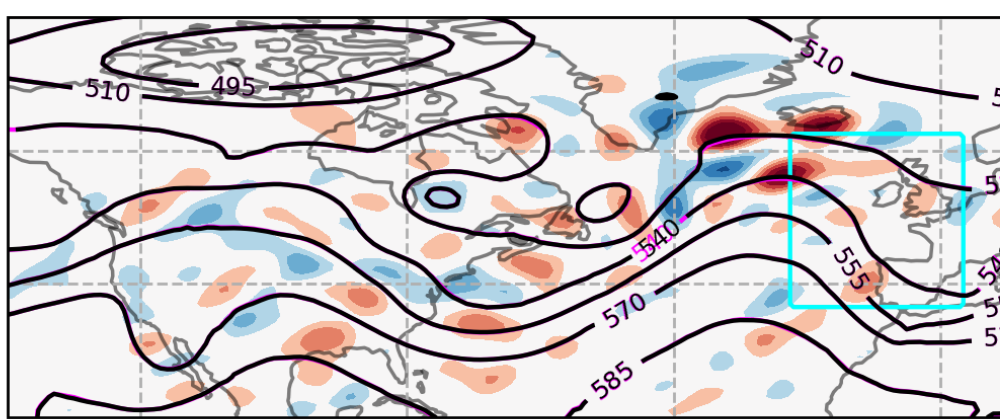
$$x^{i+1} = x^i - \eta \left( \frac{\partial L}{\partial x_0} \right)^i$$

- Optimal perturbation calculation is not restricted to linear dynamics (e.g., adjoints); it captures all nonlinear effects present in the ML model
- Useful for examining how perturbations to sensitive areas evolve in space and time and over different regions

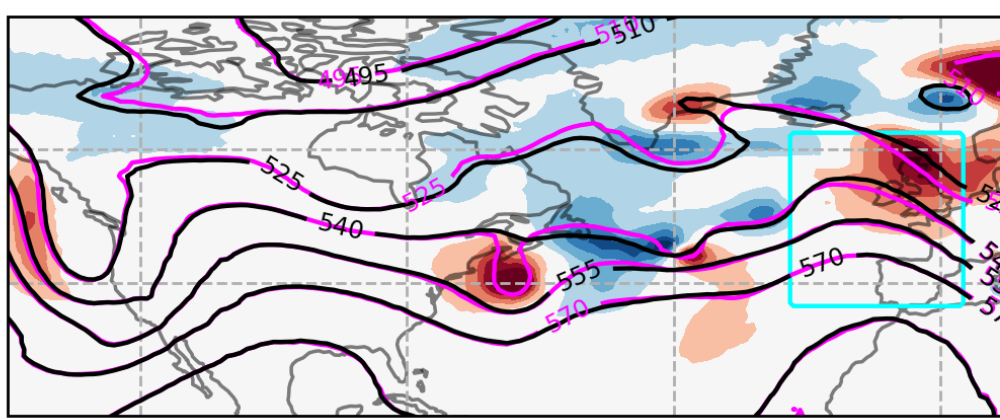


# Z500 Perturbation Evolution

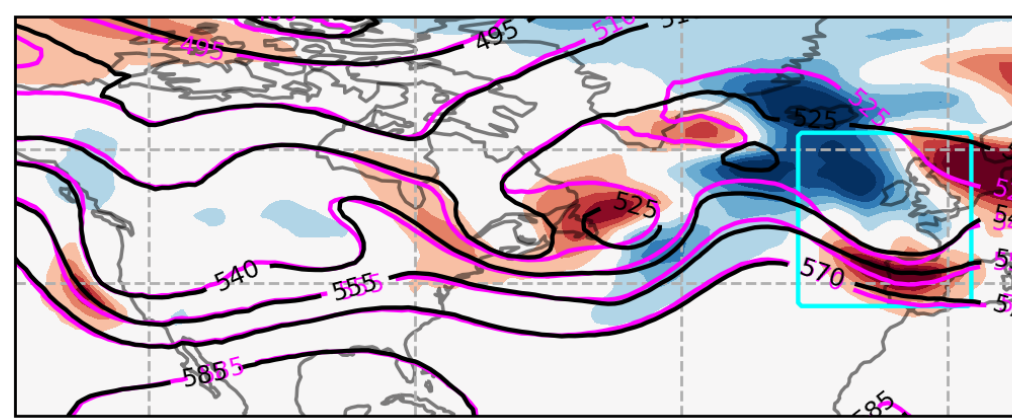
Original forecast (magenta), Optimal forecast (black), and Optimal minus Original (shading) (dam)  
 (a) 1800 UTC 13 Feb 2026 ( $t = 0$  h)      (b) 0600 UTC 15 Feb 2026 ( $t = 36$  h)



(c) 0600 UTC 17 Feb 2026 ( $t = 84$  h)

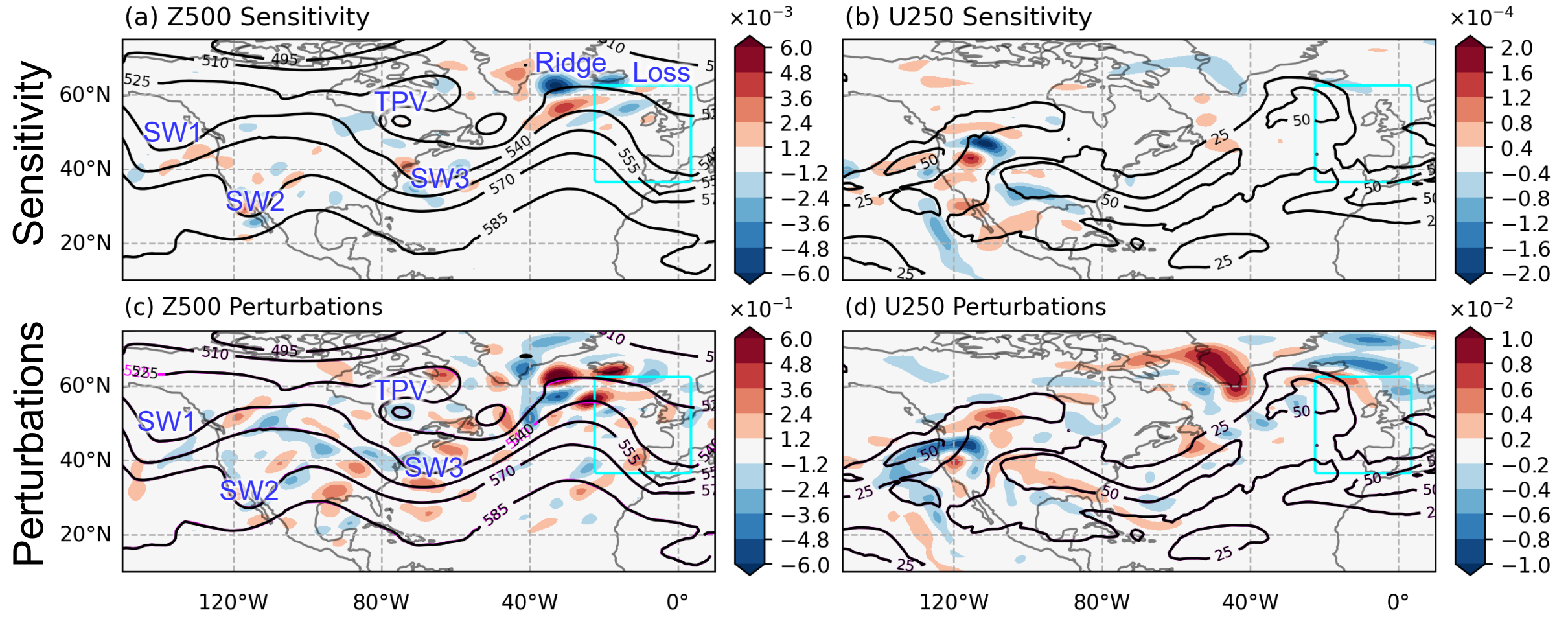


(d) 1800 UTC 18 Feb 2026 ( $t = 120$  h)



Largest initial perturbations are near the ridge, followed by rapid growth in the waveguide and SW2 & 3

# Comparing Perturbations and Sensitivity

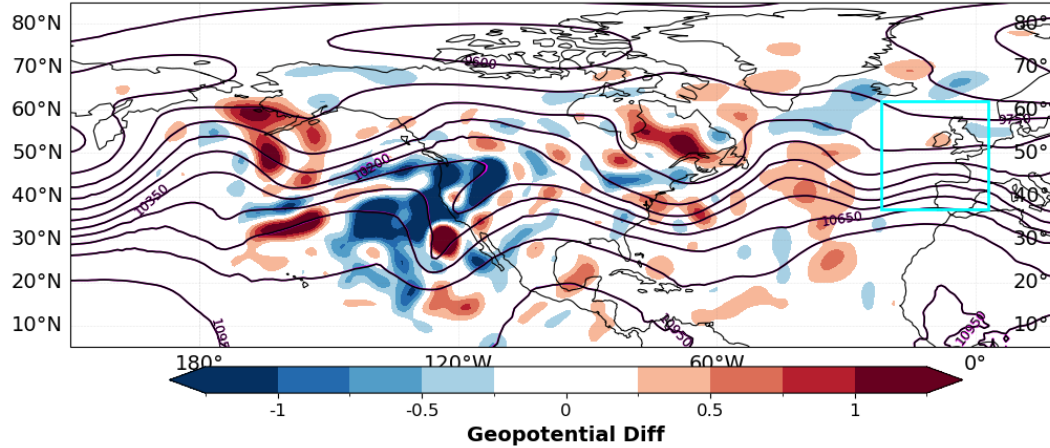


- Perturbations resemble negative of sensitivity (sensitivity is up-gradient, optimal perturbations are down-gradient)
- Patterns change during the iterations due to nonlinearities and higher-order effects

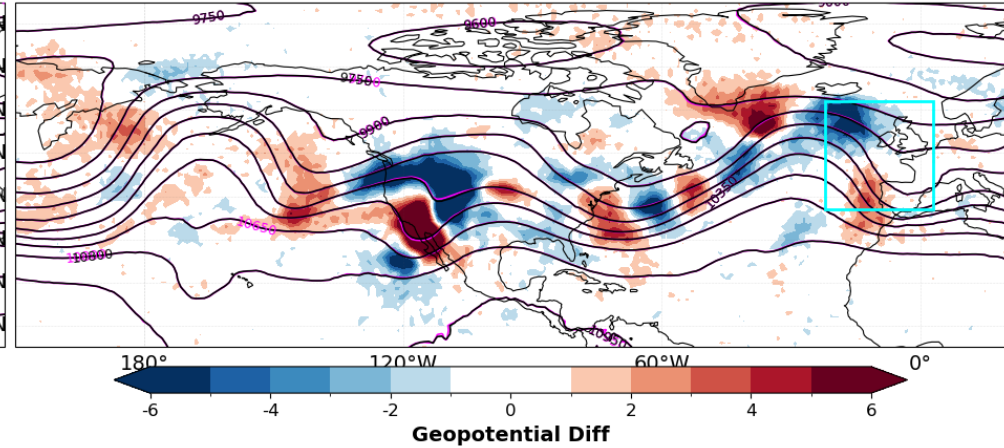
# 500-hPa GHT Initialized at 1800 UTC 12 Feb. (6 day)

Geopotential Height forecast (magenta), analysis (black),  
optimal perturbation (shading) (m)

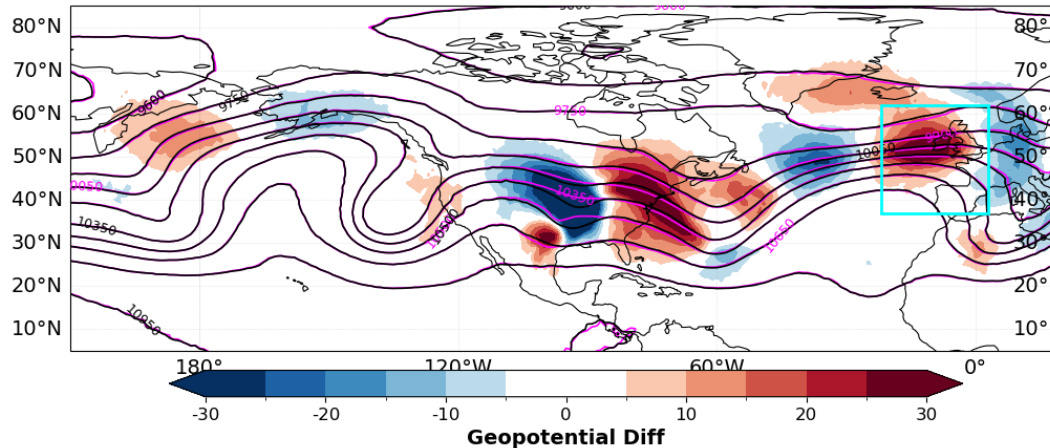
1800 UTC 12 February 2026 (t=0h)



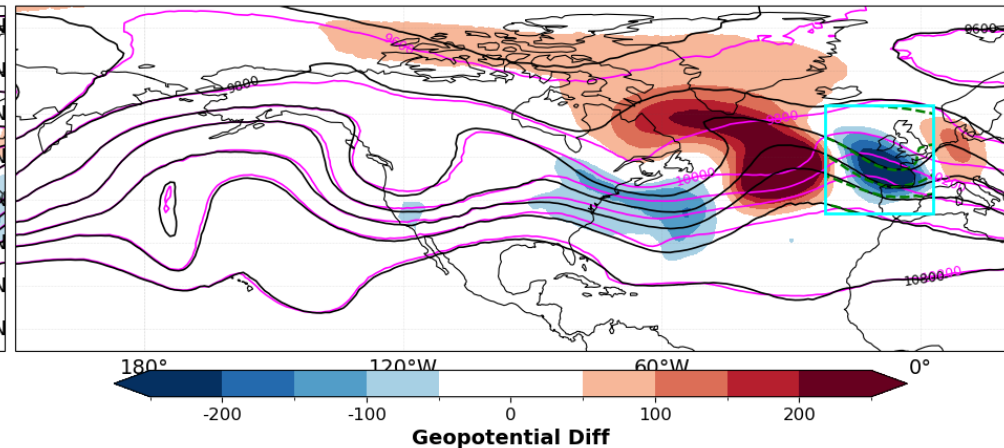
1800 UTC 13 February 2026 (t=24h)






0600 UTC 15 February 2026 (t=60h)



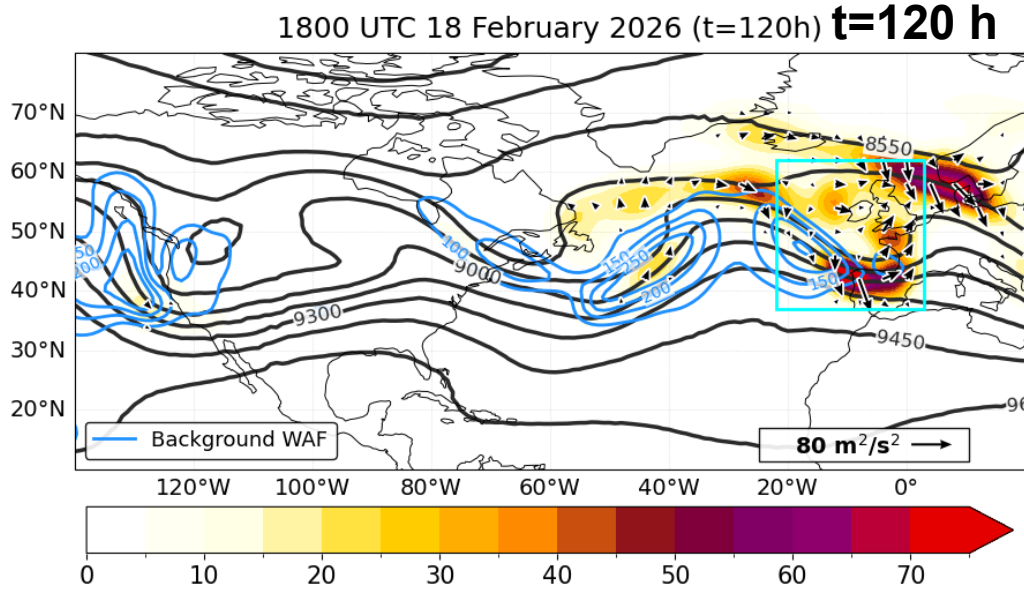
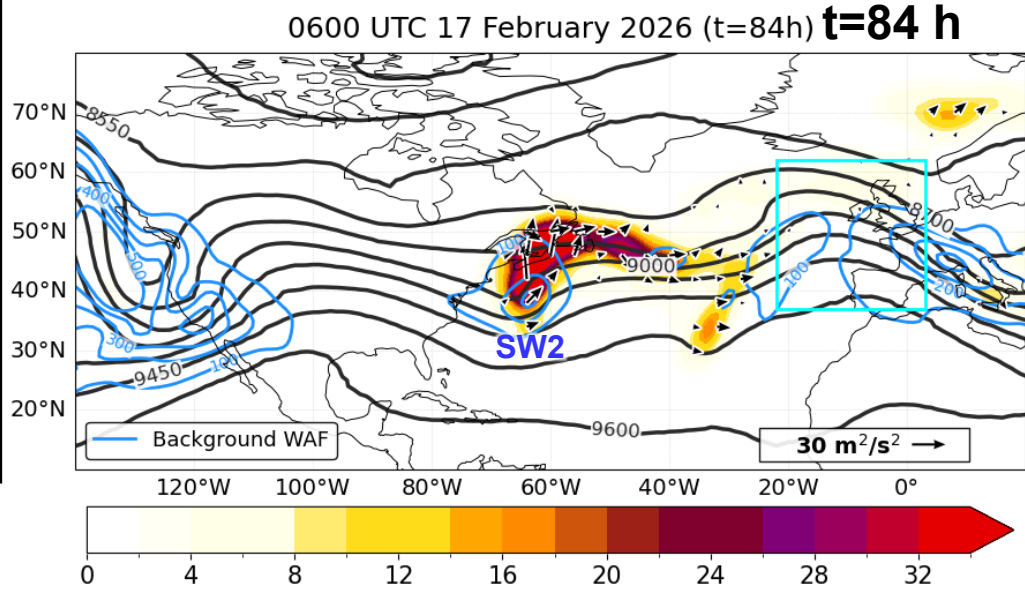
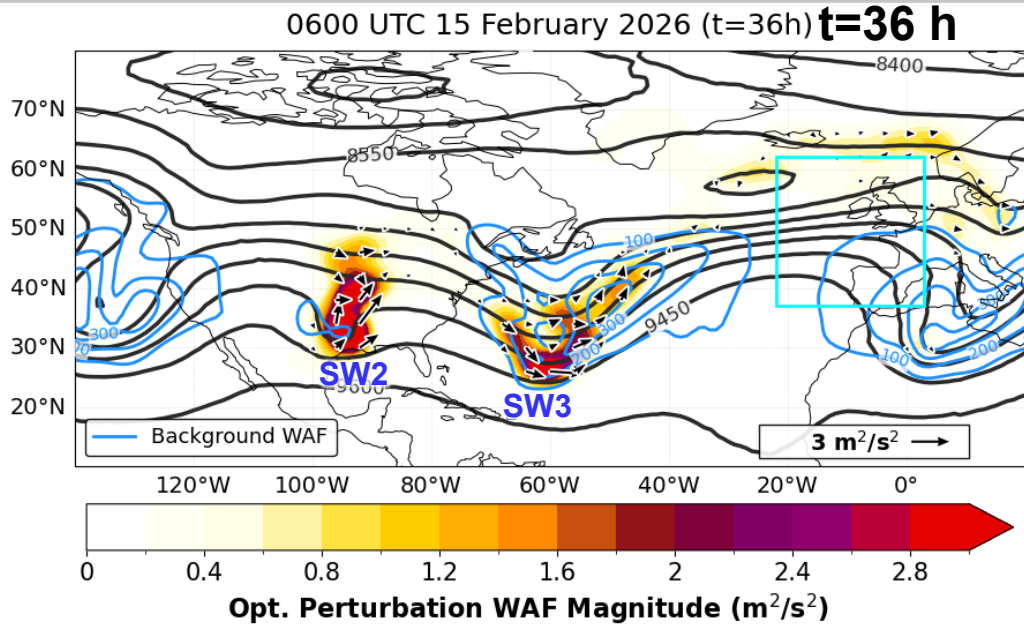
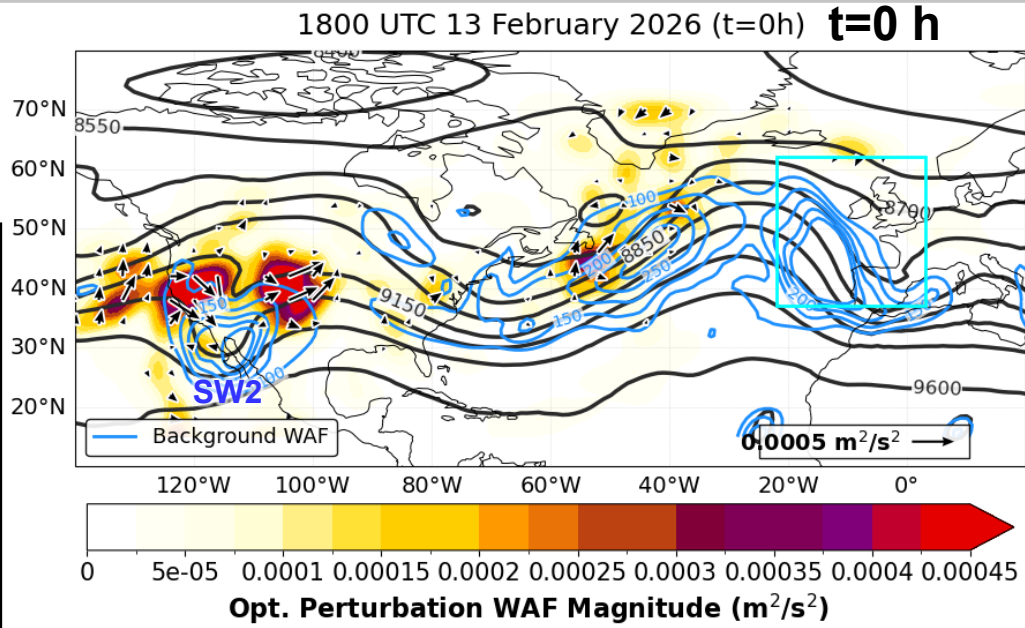
1800 UTC 18 February 2026 (t=144h)



# Optimal Perturbation Wave Activity Flux (WAF)

300-hPa heights ———  
 Pert. WAF magnitude   
 Pert. WAF vectors   
 Forecast WAF mag. 

- Wave activity flux (WAF) (Takaya-Nakamura 2001) identifies Rossby wave packets & propagation direction
- Perturbation WAF acts to reinforce background Rossby wave packets, extract energy from background flow, and disperse energy downstream



# Optimal Perturbation Takaya-Nakamura Wave Activity Flux

$$W_x = \frac{p \cos \phi}{2|U|} [U(v'^2 - \psi' v'_x) + V(-u' v' + \psi' u'_x)]$$

$$W_y = \frac{p \cos \phi}{2|U|} [U(-u' v' + \psi' v'_y) + V(u'^2 + \psi' u'_y)]$$

W: Horizontal Wave Activity Flux vector ( $W_x$ ,  $W_y$ )

p: Pressure level (normalized by 1000 hPa)

$\phi$ : Latitude

U = (U, V): Basic state (background) wind vector, with magnitude |U|

( $u'$ ,  $v'$ ): Actual (total) perturbation wind components (includes both geostrophic and ageostrophic flow)

$\psi' = \Phi' / f$ : Perturbation geostrophic streamfunction (where  $\Phi'$  is the geopotential anomaly and f is the Coriolis parameter)

Subscripts (x, y): Partial spatial derivatives in the East-West (zonal) and North-South (meridional) directions